ELSEVIER

Coordination Chemistry Reviews
210 (2000) 203–250

COORDINATION CHEMISTRY REVIEWS

www.elsevier.com/locate/ccr

Bicyclic and tricyclic bis(amido)cyclodiphosph(III)azane compounds of main group elements

Lothar Stahl *

Department of Chemistry, University of North Dakota, Grand Forks, ND 58202, USA

Received 21 October 1999; accepted 24 January 2000

Contents

* Tel.: +1-701-7772242; fax: +1-701-7772331.
E-mail address: lothar.stahl@mail.chem.und.nodak.edu (L. Stahl).

PII: S0010-8545(00)00312-X

Abstract

The coordination chemistry of bis(amido)cyclodiphosph(III)azanes as dinegative chelating *N*-donor ligands for main-group elements is reviewed. The subject is introduced by way of an overview of convenient syntheses for bis(amino)cyclodiphosph(III)azanes and a discussion of their structures, followed by classifications of the ligands and their compounds by structure type. Detailed descriptions of syntheses and structures of bicyclic and tricyclic main-group bis(amido)cyclodiphosph(III)azane compounds, organized by groups, constitute the main part of the discussion. A summary of structural trends and potential applications concludes the review.

Keywords: Cyclodiphosph(III)azane; Diazadiphosphetidine; Bis(amido) compounds; Heterocube; Heterobicycle; Heterotricycle

1. Introduction

While trying to synthesize catalytically-active early transition metal bis(amido) compounds, we were in need of chelating polyhapto amide ligands that could create a tetrahedral coordination environment [1] about these large metals. Because reactivity tests on homogeneous catalysts require an almost iterative approach to ligand design, we were particularly interested in molecules that are easy to synthesize and to modify.

Although nitrogen forms more ligands — either in the form of neutral amines or anionic amides — than all other donor atoms combined, few of them met these

basic requirements [2]. Conventional chelating bis(amides), linked by ethylene or *o*-diphenylene for example, were unsuitable because their bite is too small to effectively stabilize the early transition metals and lanthanides monomerically and tetrahedrally. A tetrahedral or pseudotetrahedral coordination environment and the *cis*-disposition of the metal's monodentate ligands, however, are necessary conditions for active catalysts.

Our dissatisfaction with established ligands and the need for uniqueness in an area of many patent barriers led us to investigate alternative amide ligands. We settled on a class compounds that is well known to main-group chemists, but rarely used by transition-metal chemists, viz. inorganic nitrogen heterocycles [3]. These molecules come in an immense variety of shapes and sizes and are formed by all metalloids and many nonmetals. The structural requirements on the ligand mandated bowl-shaped molecules with strong, covalent E–N bonds. Aware of the highly successful main-group coordination chemistry of bis(amido)cyclodisilazanes [4,5], we thought that the isoelectronic bis(amido)cyclodiphosph(III)azanes might have an equally rich coordination chemistry.

Phosphorus and nitrogen form compounds of greater structural diversity than any two congeners in the periodic table. Of these molecules the phosphazenes have attracted by far the most attention, because of their role as precursors for P–N polymers and hybrid (organic–inorganic) materials [6,7].

Phosphazanes, both cyclic [8,9] and acyclic [10] ones, however are also an established class of P–N compounds and are known for their stability and ease of synthesis. Cyclodiphosph(III)azanes were first reported by Michaelis and Schroeter in the late 19th century [11], but only fully characterized in the 1960s [12]. As late as 1969 the four-membered ring structure of some cyclodiphosph(III)azanes was disputed [13]. The verification of the central $(P–N)_2$ ring by X-ray studies in 1971 had a catalytic effect on the research interests in cyclodiphosph(III)azanes [14]. Much synthetic and mechanistic work in the past three decades has led to a good understanding of the structures and reactivities of these saturated phosphorus–nitrogen heterocycles [15–20].

Krishnamurthy and others [21,22] have used cyclodiphosphazanes as ligands for transition metals, but these studies focused exclusively on the P-donor properties of these molecules — a bias that may stem from aminophosphines. In the course of our studies on transition metal cyclodiphosphazanes compounds, we realized that few main group derivatives of bis(amido)cyclodiphosphazanes existed. We therefore began exploring main-group derivatives of bis(amido)cyclodiphosphazanes, the first of which had been reported as late as 1983 [20]. In the following pages the syntheses and structures of bicyclic and tricyclic bis(1°-amido)cyclodiphosph(III)azane compounds with main-group element incorporation will be reviewed.

2. Definitions, conventions and nomenclature

Bis(1°-amino)cyclodiphosph(III)azanes (**A**) are the formal [2 + 2] cycloaddition products of aminophosphazenes, R(H)NP=NR (also called amino(imino)-

phosphines). Their characteristic structural feature is a central four-membered ring of alternating trivalent phosphorus and nitrogen atoms. Each atom bears one exocyclic substituent; those on the nitrogen atoms lie approximately in the plane of the ring, while the amino-substituents of the phosphorus atoms are almost perpendicular to it. This disposition of the P-substituents makes *cis*- and *trans*-isomers possible, although frequently only one isomer is isolated.

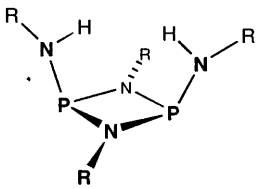

A

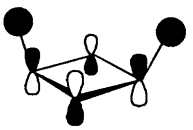

B

Cyclodiphosph(III)azanes are related to cyclodiphosph(V)azanes and cyclophosphazenes, but differ from both in having P(III), rather than P(V), centers and from the latter in having three-coordinate, rather than two-coordinate, nitrogen atoms.

The lack of a uniform and generally accepted nomenclature for cyclic P–N molecules makes the unambiguous designation of these compounds difficult and has on occasion led to confusion in the literature. The most common name for these four-membered heterocycles is diazadiphosphetidine. Because this naming system cannot be extended to higher homologues, and because it is derived from organic nomenclature, I will use the name cyclodiphosph(III)azane consistently in this review.

The numbering scheme for cyclodiphosph(III)azanes is unambiguous, however, the nitrogen atoms being the 1 and 3 atoms, while the phosphorus atoms are the 2 and 4 atoms of the ring. Ring substituents are numbered in order of their priority, the substituents of highest priority being given the lowest number.

Although, in principle, almost any atom or organic group can serve as exocyclic substituents of cyclodiphosph(III)azanes, the ring-nitrogen substituents are always alkyl, aryl, or silyl. The exocyclic P-substituents are much more variable, however, and they may be halogens, alkyl, aryl, alkoxy, and amino groups. The cyclodiphosph(III)azanes discussed herein bear silyl or hydrocarbyl substituents on the imino-nitrogens, and, with the exception of some synthetic intermediates, primary amines on the phosphorus atoms.

The core structure of bis(amino)cyclodiphosphazanes is thus an inorganic N–(P–N)$_2$–N bowl with four organic substituents, as shown in **A**. To facilitate the discussion of these heterocycles, we classify them as shown in Scheme 1.

Homosubstituted bis(amino)cyclodiphosph(III)azanes have identical organic substituents on all four nitrogen atoms. An example is [^{t}Bu(H)N(^{t}BuNP)$_2$N(H)^{t}Bu] (**1**), with the full name 1,3-di-*tert*-butyl-*cis*-2,4-di-*tert*-butylaminocyclodiphosph-(III)azane.

Heterosubstituted cyclodiphosph(III)azanes have two or more different organic substituents and can exist as symmetrically- and asymmetrically-heterosubstituted molecules. An example of a symmetrically-heterosubstituted cyclodiphosph(III)azane is [Ph(H)N(^{t}BuNP)$_2$N(H)Ph] (**5**). Here the substituents on the imino nitrogens are identical, viz. *tert*-butyl, but are different from those on the amino nitrogens, viz. phenyl.

Asymmetrically-heterosubstituted bis(1°-amino)cyclodiphosph(III)azane [^{t}Bu(H)-N(^{t}BuNP)$_2$N(H)Ph] (**7**), with the full name 1,3-di-*tert*-butyl-*cis*-2-anilino-4-*tert*-butylaminocyclodiphosph(III)azane, have different amino-nitrogen substituents, viz. *tert*-butyl and phenyl.

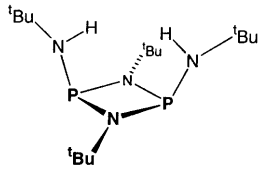

1

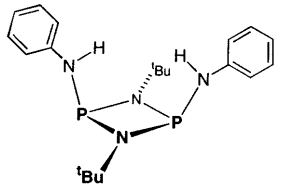

5

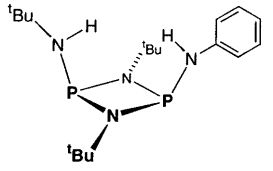

7

Scheme 1.

3. Scope

This is a review of compounds in which main-group metals, metalloids and nonmetals are coordinated by bis(amido)cyclodiphosph(III)azanes via the amido nitrogen atoms. In the ensuing bicyclic and tricyclic compounds the bis(amido)cyclodiphosph(III)azane can be considered a dinegative ligand, which chelates the main-group element(s) in a di- or trihapto fashion.

Reviews on cyclodiphosph(III)azanes have appeared at irregular intervals [8,9], but none of them has explicitly discussed the coordination chemistry of bis(amino)cyclodiphosph(III)azanes as *N*-donor ligands. Transition metal compounds of bis(amido)cyclodiphosph(III)azanes and main group derivatives of bis(amido)cyclodiphosph(V)azanes or of amidocyclophosphazenes are not included in this review. The literature is covered through December 1999.

4. Bis(amino)cyclodiphosph(III)azanes

4.1. Syntheses and structures of bis(amino)cyclodiphosph(III)azanes

Because the structure of any coordination compound is closely related to the structure of its ligand, I will begin the discussion with a short review on ligand syntheses, and some configurational and conformational aspects of these molecules. Depending on the structure type, bis(amino)cyclodiphosph(III)azanes can be rationally synthesized by one of three routes.

Route 1: Symmetrically-homosubstituted bis(amino)cyclodiphosph(III)azanes are best prepared by the interaction of PCl_3 with a five-fold excess of a primary amine [12]. This procedure is not only the easiest, but also one of the oldest syntheses for cyclodiphosph(III)azanes. Typical examples of this type of reaction, which usually provides the heterocycle in very good yields, are given in Eqs. (1) and (2) of Scheme 2. The product is conveniently purified by fractional crystallization, but other methods, such as vacuum distillation, have also been used. The excess amine serves as a Brønsted base for the HCl generated in the reaction, but if the primary amine is expensive, triethylamine may be used as well.

Fig. 1 shows a drawing of the solid-state structure of the very common symmetrically-homosubstituted 1,3-di-*tert*-butyl-*cis*-2,4-di-*tert*-butylaminocyclodiphosph(III)azane (**1**) [23]. One of the most noteworthy features of this molecule is the puckered $(P–N)_2$ ring — a topic that will be discussed in greater detail in Section 4.2.

The perspective view emphasizes depth and span of the molecule, which are sufficient to accommodate even the largest of elements (the distance between the amino-nitrogens is ca. 4.1 Å). This molecule has crystallographic symmetry 2, with endocyclic and exocyclic P–N bonds of 1.725(2) and 1.664(2) Å, respectively. As with most pristine bis(amino)cyclodiphosph(III)azanes, the exocyclic P–N bonds are shorter than the endocyclic ones. Phosphorus–nitrogen bonds in cyclodiphosph(III)azanes fall in the range 1.65–1.75 Å and are thus somewhat shorter than

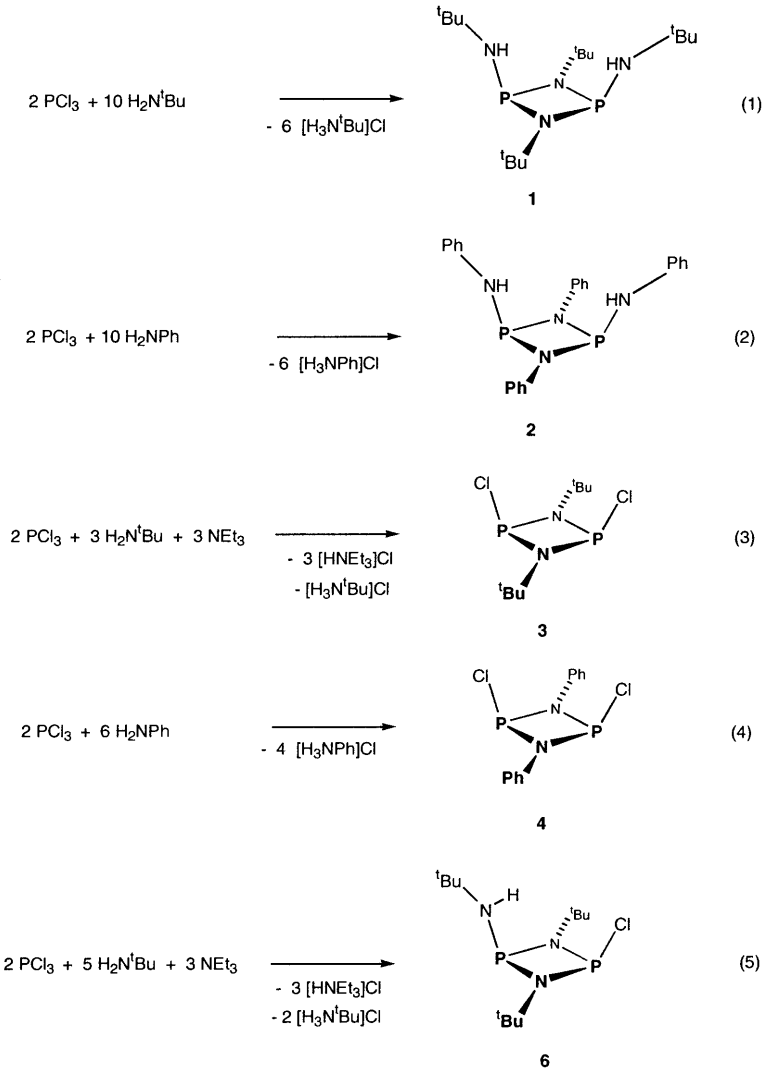

Scheme 2.

P–N single bonds, but not as short as P–N double bonds [24]. Selected bond lengths for **1**, as for all cyclodiphosph(III)azanes discussed in this review, are summarized in Table 1.

Another example of a symmetrically-homosubstituted bis(amino)cyclodiphosph(III)azane is $[Ph(H)N(PhNP)_2N(H)Ph]$ (**2**), which can be synthesized either by the transamination of tris(diethylamino)phosphine with aniline [25], or the addition of excess aniline to PCl_3, as shown in Eq. (2). While no X-ray structural data are available for **2**, the diagnostic ^{31}P-NMR data confirmed that the anilino substituents adopt the *cis*-configuration. This 1,3-diphenyl-*cis*-2,4-

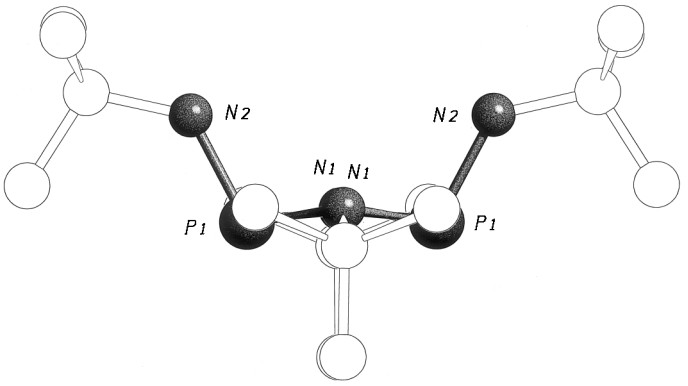

Fig. 1. Solid-state structure of [^{t}Bu(H)N (^{t}BuNP)$_2$N(H)^{t}Bu] (**1**).

dianilinocyclodiphosph(III)azane is sparingly soluble in most organic solvents, and thus synthetically not as useful as the aliphatic or mixed aliphatic/aromatic ligands.

Route 2: Heterosubstituted bis(amino)cyclodiphosph(III)azanes cannot be synthesized rationally in one-step procedures. Symmetrically-heterosubstituted cyclodiphosph(III)azanes are best prepared from 1,3-di-*tert*-buty-*cis*-2,4-dichlorocyclodiphosph(III)azane (**3**) [26] or 1,3-diphenyl-*cis*-2,4-dichlorocyclodiphosph(III)azane (**4**) [27,28]. The latter one of these has been made by no less than five different routes, the most convenient one of which is shown in Eq. (4). The reported synthesis for **3** is unnecessarily complex, and a more efficient synthesis for this molecule is given in Eq. (3) [29].

Both of these dichloro derivatives were characterized by single-crystal X-ray techniques, and the *cis*-configuration of the chloro substituents was confirmed in each case. A perspective view of the solid-state structure of **3** [30], which emphasizes the almost planar $(P–N)_2$ ring conformation, appears in Fig. 2.

The phosphorus nitrogen bonds in these dichlorocyclodiphosph(III)azanes (**3** and **4**) are identical, but they are slightly shorter than those in the amino-substituted

Table 1
Selected bond lengths (in Å) for some cyclodiphosph(III)azanes

Molecule	P–N (*endo*) (mean)	P–N (*exo*) (mean)	P–Cl	P···P
^{t}Bu(H)N(^{t}BuNP)$_2$ N(H)^{t}Bu (**1**)	1.726(2)	1.664(2)	–	2.600(2)
Cl(^{t}BuNP)$_2$Cl (**3**)	1.689(9)	–	2.105(7)	2.53
Cl(PhNP)$_2$Cl (**4**)	1.695(10)	–	2.087(8)	–
Ph(H)N(^{t}BuNP)$_2$ N(H)Ph (**5**)	1.726(2)	1.689(2)	–	2.5829(13)
^{t}Bu(H)N(^{t}BuNP)$_2$Cl (**6**)	1.674(3) to P–Cl, 1.748(3) to P–N	1.659(3)	2.2047(13)	2.5915(11)

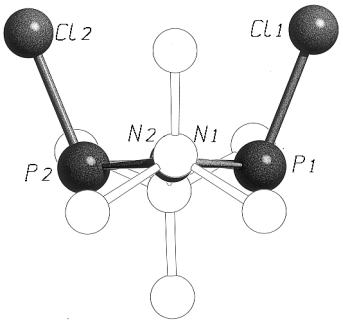

Fig. 2. Solid-state structure of [Cl(^{t}BuNP)$_2$Cl] (**3**).

ligands **1** and **5**. The major structural difference between the dichloro species is the (P–N)$_2$ ring, which is slightly puckered in **3**, but planar in **4**, suggesting that the conformation of the (P–N)$_2$ ring may depend on the imino-nitrogen substituents.

Substitution of the chlorine atoms of dichlorocyclodiphosph(III)azanes with amino groups can be accomplished in two ways. The easiest of these is the treatment of a dichlorocyclodiphosph(III)azane with two equivalents of a primary amine and two equivalents of triethylamine, as shown in Eq. (6) of Scheme 3. This reaction works well only for acidic amines, like pyrazoles and aniline, however, and in the latter case provides 1,3-di-*tert*-butyl-*cis*-2,4-dianilinocyclodiphosph(III)azane (**5**) [31]. In a similar fashion the ring can be substituted with a wide variety of other aromatic amines.

The second, and more general method of ring substitution, is the reaction of **3** or **4** with two equivalents of the corresponding lithium amide, shown in Eq. (7). This procedure gives the cleanest products, but it does require one additional step.

The solid-state structure of **5** is shown in Fig. 3. Here, as in **1**, the (P–N)$_2$ ring is puckered, in contrast to the almost planar ring for the imino-aryl substituted molecules **2** and **4**. Although this may suggest that the imino, rather than the amino-substituents, determine the ring conformation, other factors probably also play a role. An interesting structural feature of this symmetrically-heterosubstituted ligand is the perpendicular disposition of the phenyl rings with respect to the heterocycle, from which it can be inferred that the amino-nitrogen and phosphorus lone pairs are orthogonal. Possible reasons for these structural details are discussed in Section 4.2.

Route 3: Asymmetrically-heterosubstituted bis(amino)cyclodiphosph(III)azanes, like [^{t}Bu(H)N(^{t}BuNP)$_2$Cl] (**6**), were prepared in a similar one-step reaction by the appropriate stoichiometric adjustments [29]. This monochloro species is a good starting material for ligands with three *tert*-butyl substituents. Recent improvements (Eq. (5)) on the published procedure have allowed the isolation of this molecule in yields exceeding 70% [31].

Fig. 4 shows a view of the solid-state structure of **6**, which demonstrates the *cis*-configuration of the two phosphorus substituents Cl and N(H)^{t}Bu [31]. While the (P–N)$_2$ ring is puckered, this distortion is less severe than in **1**. Perhaps due to

steric crowding, the unique P–Cl bond is much longer (2.2047(13) Å) than those in the dichloro species **3** (2.105(7) Å) and **4** (2.087(7) Å). The endocyclic P–N bonds are unsymmetrical (1.674(3) and 1.748(3) Å), with those to P–Cl being shorter.

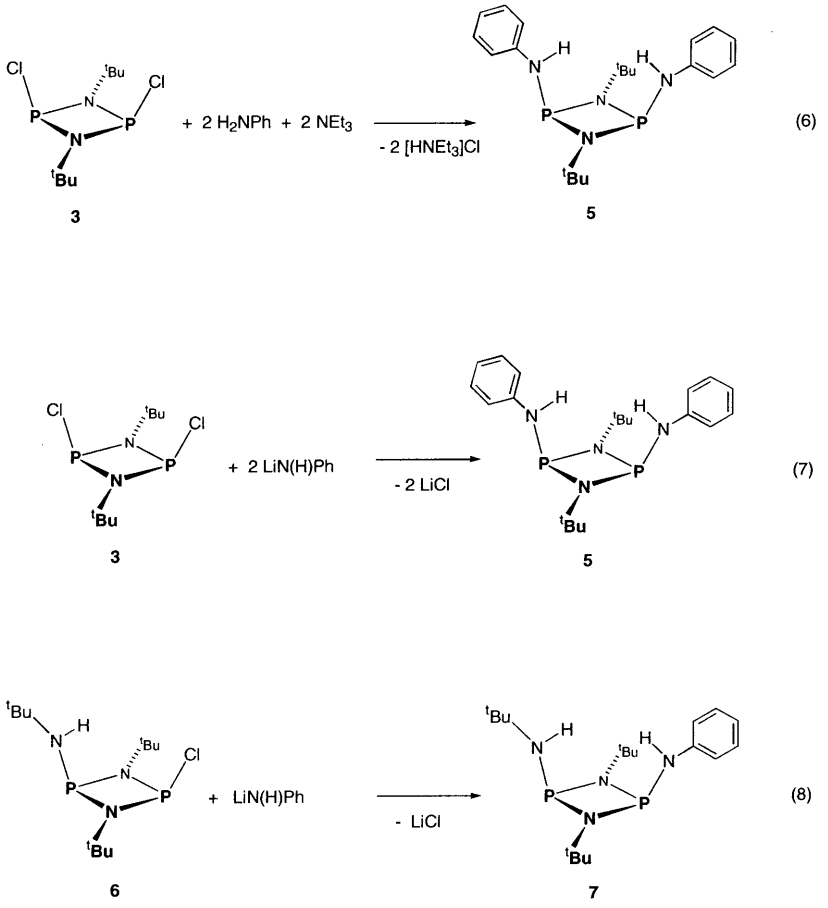

Scheme 3.

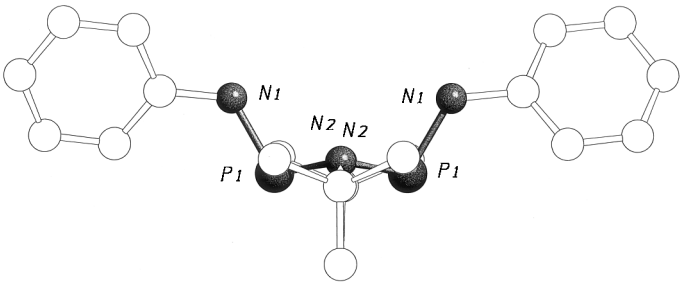

Fig. 3. Solid-state structure of [Ph(H)N('BuNP)$_2$N(H)Ph] (**5**).

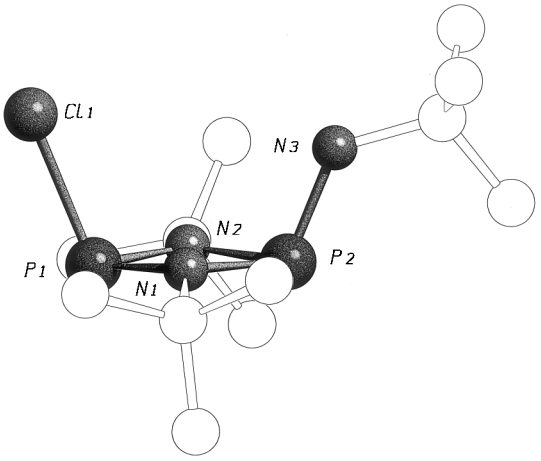

Fig. 4. Solid-state structure of [^{t}Bu(H)N(^{t}BuNP)$_2$Cl] (**6**).

Treatment of **6** with one equivalent of lithium anilide (Eq. (8)) affords the asymmetrically-heterosubstituted bis(amino)cyclodiphosph(III)azane **7**. Aminolysis of the P–Cl bond with aniline in the presence of triethylamine is not useful route for this transformation, as it leads to transamination. The *cis*-configuration of the phosphorus substituents in **7** was deduced from ^{31}P-NMR data.

4.2. Cis/trans-isomerism and ring conformation

Because only *cis*-cyclodiphosph(III)azanes can serve as chelating ligands, it is desirable to be able to predict the ligand's configuration prior to its synthesis.

Like their homocyclic analogues — cyclobutanes — cyclodiphosph(III)azanes can exist as *cis*- and *trans*-isomers. X-ray structural and solution ^{31}P-NMR studies have allowed the isomer assignment of virtually all known (ca. 100) cyclodiphosph(III)azanes. Although both isomers occur in approximately equal amounts, there is a small majority of *cis*-isomers. In the solid-state, only the thermodynamically preferred *cis*-isomer is encountered, but in solution many cyclodiphosph(III)azanes are present in appreciable concentrations as both isomers, demonstrating that their energy differences are small.

Isomer preference does not follow obvious steric or electronegativity trends and is thus not easy to predict. There is, however, a very clear trend in the ring conformations of these isomers: *trans*-isomers have planar or almost planar $(P–N)_2$ rings, while *cis*-isomers have puckered rings.

Keat suggested that the source of the puckering is the lone-pair repulsion on adjacent phosphorus and nitrogen atoms [9], which is lessened for pyramidalized imino-nitrogen atoms. Although this is a plausible account, it fails to explain why *cis*-2,4-dihalocyclodiphosphazanes are less puckered than 2,4-diamino-cyclodiphosph(III)azanes, or why *trans*-isomers are planar or almost planar.

A more recent theoretical study has addressed the configurational and ring-conformational preferences of cyclodiphosph(III)azanes in greater detail [32]. These molecular-orbital calculations (3-21G* and MNDO/2) were done on cyclodiphosph(III)azanes with small substituents, thereby eliminating steric effects. The authors concede that for very large ring-substituents, steric effects alone may determine the molecular configuration.

At both levels of calculation, the *cis*-isomers were found to have lower enthalpies of formation than the *trans*-isomers. The energy differences between isomers were small, however, ranging from 4 to 40 kJ mol^{-1}, with most compounds being at the lower end of this range. These results are in good agreement with the slight majority of *cis*-isomers and the presence of both isomers in the solution-phase NMR spectra of some cyclodiphosph(III)azanes.

Because of orbital mixing, the source of the greater stability of *cis*-isomers could not be determined. The thermodynamic trends closely parallel ring puckering, however, with cyclodiphosph(III)azanes having the greatest thermodynamic preference for the *cis*-isomer, also having the most puckered ring. Based on these results the authors concluded that whatever favors puckering also favors the *cis*-isomer and vice versa and chose ring conformation as measure of configurational preference.

The ring conformation, in turn, is mainly determined by the energy of the HOMO of the molecule, which is, in essence, the HOMO of the naked $(P–N)_2$ ring. The energy of this π^* orbital (shown as **B**) is raised by electron releasing substituents and lowered by electron withdrawing substituents. Ring puckering decreases the negative overlap of the HOMO and is thus most prominent for rings with electron-donating substituents. Electron-releasing substituents on the $(P–N)_2$ ring thus predispose the ligand to puckering and the *cis*-configuration.

This model is reasonably straightforward for substituents having only σ-interactions with the ring, but it is more complex if substituents bearing lone pair electrons are present. For amine substituents this destabilizing π-interaction can be turned off, by rotating the lone pair until it is perpendicular to the π-orbital of the ring. This is nicely demonstrated by the disposition of the phenyl groups in **5** (Fig. 3). Ring substituents with more than one lone pair, like oxygen and halogens, however, create additional interactions whose effect on the energy of the orbital cannot be predicted easily.

While these theoretical studies provide important insight into the source of ring puckering, they are too complex to be a guide for synthetic chemists. A set of empirical rules stated by Norman is much more useful for this purpose [27]. The following is a shortened version of these rules, as they apply to the cyclodiphosph(III)azanes discussed in this review:

- 2,4-Dihalocyclodiphosph(III)azanes are always *cis*, irrespective of the imino--substituents.
- 1,3-Diaryl-2,4-bis(amino)cyclodiphosph(III)azanes have the *cis*-geometry as long as at least one of the P-substituents is a primary amine.
- 1,3-Dialkyl-2,4-bis(amino)cyclodiphosph(III)azanes always exhibit the *cis*-geometry.

4.3. Cis/trans-isomer interconversion

As suggested by their configurational preferences, most cyclodiphosph(III)azanes are thermodynamically more stable as *cis*-isomers. The *trans*-isomer is often the kinetic product, however, and this raises the question how *trans*- and *cis*-isomers interconvert. The most plausible mechanism of *trans*/*cis*-isomerization is a pyramidal inversion at phosphorus, especially since such inversions are a well-known mode of configurational change for trivalent Group 15 compounds [33].

More recent theoretical calculations suggest that edge inversions, i.e. inversions at the imino-nitrogen, have similar activation energies [34]. In some cases the calculated activation energies for edge inversion were, in fact, found to be lower than those for vertex (P) inversion.

Both vertex and edge inversions occur on intact cyclodiphosph(III)azanes. By contrast, a third conceivable mechanism of interconversion involves cycloreversion of the cyclodiphosph(III)azane, either partial or complete. Bond rotation or recombination of these species, respectively, can then lead to a change of geometrical isomer [27]. Such ring-opening reactions (cycloreversions) are known for cyclodiphosph(III)azanes, especially those with bulky substituents, and this process must be considered a distinct alternative to closed-ring isomerization [35,36].

5. Bis(amido)cyclodiphosph(III)azane compounds of main group elements

5.1. Synthetic routes and structure patterns

It is a tribute to the great stability of bis(amido)cyclodiphosph(III)azane compounds that the first main-group compounds of bis(amino)cyclodiphosph(III)azanes were the products of chance syntheses [20,37]. These accidental discoveries and the lack of convenient starting materials, however, may have prevented the systematic study of bis(amido)cyclodiphosph(III)azanes as chelating *N*-donor ligands. Bis(amido)cyclodiphosph(III)azane compounds are best made by one of the following three synthetic procedures:

- Interaction of the element halide with a dilithio bis(1°-amido)cyclodiphosph(III)azane.
- Aminolysis of polar E–X bonds with a bis(1°-amino)cyclodiphosph(III)azane in the presence of a tertiary amine. This procedure is superior for the incorporation of redox-sensitive elements.
- Redox transmetallation of certain divalent Group 14 bis(amido)-cyclodiphosph(III)azanes with the corresponding element tetrachloride.

Bis(amido)cyclodiphosph(III)azane compounds synthesized by any one of these three reaction types adopt one of three basic structures.

Compounds with two chelated main-group atoms have a heterocubic structure, labeled **I** in Scheme 4, in which all corners of the cube are occupied by inorganic

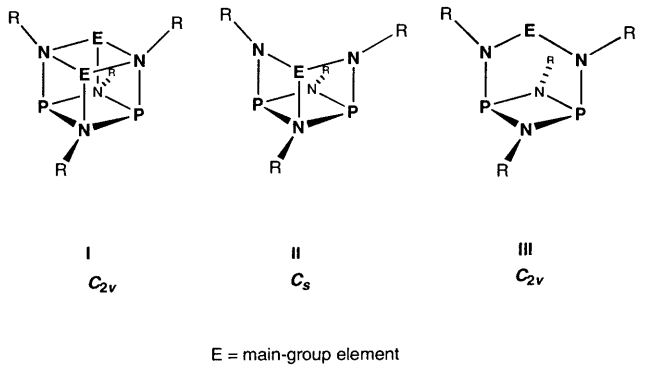

Scheme 4.

elements. Because of the substantial size differences of the corner atoms, however, the C_{2v}-symmetric heterocubes are often highly distorted.

Cyclodiphosph(III)azane compounds with one chelated element adopt one of the two idealized structures, **II** and **III**. In the C_s-symmetric **II**, the coordinated element E occupies one corner of a cube, leaving the other corner unoccupied. This type of structure is sometimes referred to as a *seco*-heterocube, on account of the 'excised' element.

In structure type **III**, however, the main-group element is coordinated above the center of the cyclodiphosph(III)azane ring. Molecules of this type have idealized C_{2v} symmetry, if the element has two identical exocyclic substituents, but C_s symmetry if the element bears two different groups. Most mono-element compounds of bis(amido)cyclodiphosph(III)azane compounds have structures that are intermediate between types **II** and **III**.

5.2. Bis(amido)cyclodiphosph(III)azane compounds of Group 1 elements

5.2.1. Lithium compounds

The successful development of a ligand's coordination chemistry is crucially dependent upon the availability of convenient starting materials. Amides can be made from neutral amines, via N–H bond cleavage with a suitable base. This process is of limited use, however, and more typically these ligands are introduced in the anionic form as alkali-metal salts.

Primary amines are not very acidic. Aliphatic amines, for example, have pK_a values around 40 [38], and only certain aromatic amines have much lower pK_a values. The proximity to the phosphorus(III) atom should not significantly enhance the acidity of the N–H moieties. Therefore only the strongest of bases, like alkyllithium reagents, are capable of quantitatively deprotonating bis(amino)cyclodiphosph(III)azanes.

Addition of ^{n}BuLi to [^{t}Bu(H)N(^{t}BuNP)$_2$N(H)^{t}Bu] in THF (Eq. (9) of Scheme 5) followed by a 3 h reflux afforded [(^{t}BuNP)$_2$(^{t}BuNLi·THF)$_2$] (**8**) [23b]. This highly crystalline, colorless solid is an excellent starting material for compounds of this

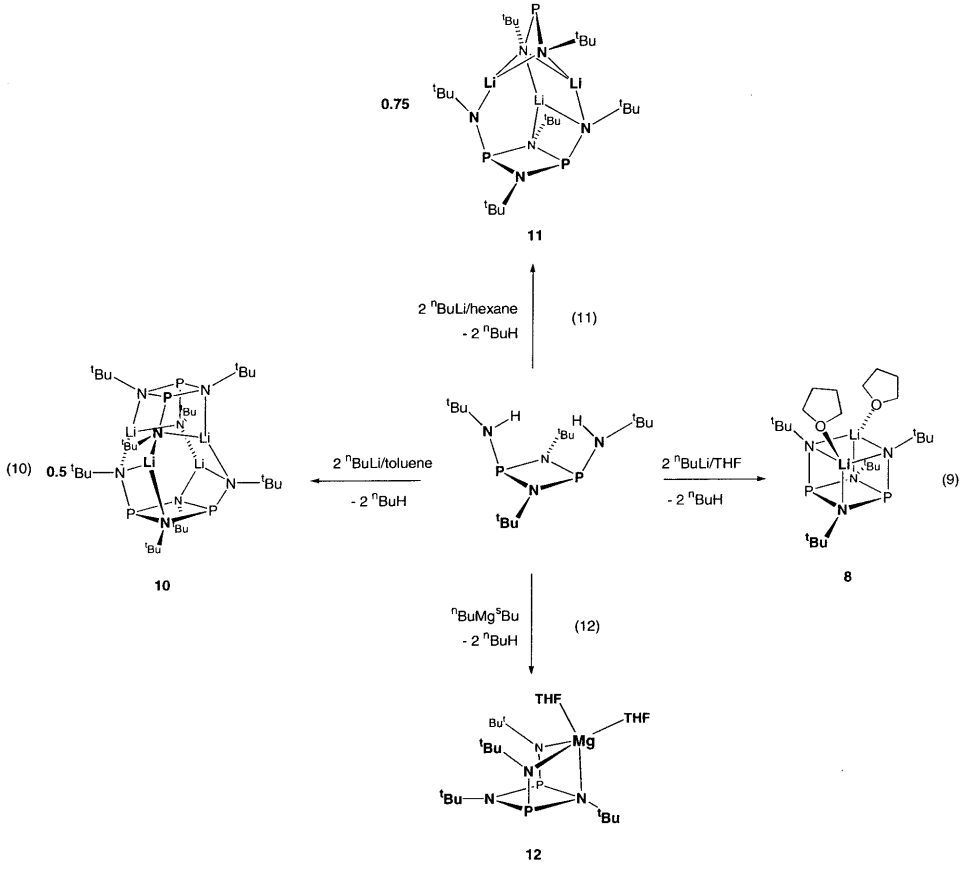

Scheme 5.

ligand. The attempted monolithiation of [^{t}Bu(H)N(^{t}BuNP)$_2$N(H)^{t}Bu] with one equivalent of ^{n}BuLi led only to the dilithio product **8**, suggesting that the heterocube is inherently more stable than two monolithio derivatives.

The solid-state structure of the C_{2v}-symmetric **8**, shown in Fig. 5, emphasizes the almost planar (P–N)$_2$ ring conformation. The endocyclic P–N bonds are longer than those in the pristine ligand (1.778(2) vs. 1.726(2) Å), but the exocyclic P–N bonds are essentially unchanged (1.651(2) vs. 1.664(2) Å). The six Li–N bonds are almost equidistant, ranging from 2.077(5) to 2.121(5) Å.

Prior to the isolation of **8**, Wright and co-workers had reported a valence-isoelectronic bismuth analogue, viz. (^{t}BuNBi)$_2$(^{t}BuNLi·THF)$_2$. This compound was not synthesized by the deprotonation of the bismuth analogue of **1** (which does not exist) with ^{n}BuLi, however, but by treating Me$_2$N(^{t}BuNBi)$_2$NMe$_2$ with ^{t}Bu(H)NLi [39].

Lithiation of the symmetrically-heterosubstituted [Ph(H)N(^{t}BuNP)$_2$N(H)Ph] afforded [(^{t}BuNP)$_2$(PhNLi·THF)$_2$] (**9**) [36], whose physical and chemical properties

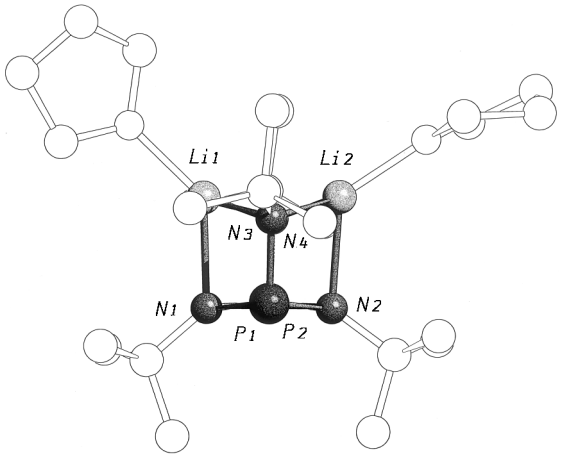

Fig. 5. Solid-state structure of [(^{t}BuNP)$_2$(^{t}BuNLi·THF)$_2$] (**8**).

are similar to those of **8**. A perspective view of this molecule, which is shown in Fig. 6, emphasizes the rhombic distortion of the heterocube along the P···P axis.

In order to isolate dilithio bis(*tert*-butylamido)cyclodiphosph(III)azanes solvent free, the diamine must be deprotonated in noncoordinating solvents, like toluene or hexanes. Chivers and co-workers discovered that the identity of the reaction product(s) depends on the order in which bis(*tert*-butylamino)cyclodiphosph-(III)azane and *n*-butyllithium are added [40]. Addition of **1** to *n*-butyllithium, for example, yielded exclusively [(^{t}BuNP)$_2$(^{t}BuNLi)$_2$]$_2$. This species is dimeric below room temperature, but it dissociates into two [(^{t}BuNP)$_2$(^{t}BuNLi)$_2$] heterocubes at ambient temperature, as shown in Scheme 6.

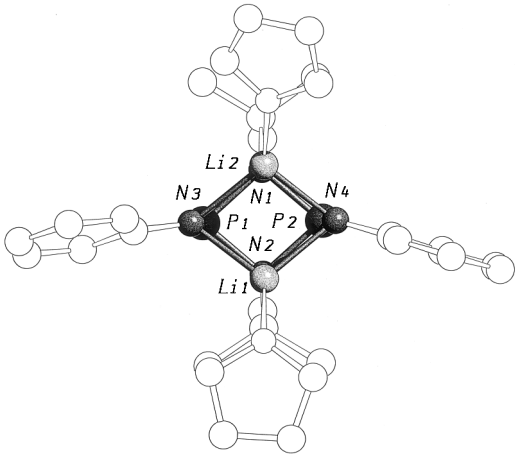

Fig. 6. Solid-state structure of [(^{t}BuNP)$_2$(PhNLi·THF)$_2$] (**9**).

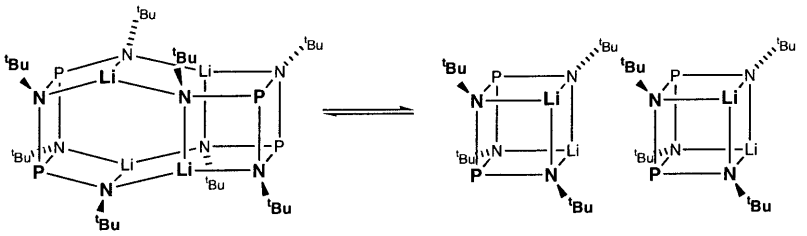

10

Scheme 6.

The reverse addition, however, produced both the dimer $[(^t\text{BuNP})_2(^t\text{BuNLi})_2]_2$ and the phosphazane cage $P_4(N^t\text{Bu})_6$, which cocrystallize in a 4:1 ratio as $[(^t\text{BuNP})_2(^t\text{BuNLi})_2]_2 \cdot 0.25\ P_4(\text{NtBu})_6 = (\mathbf{10} \cdot 0.25P_4N_6)$ (the monoclinic unit cell contains four $[(^t\text{BuNP})_2(^t\text{BuNLi})_2]$ dimers and one molecule of the tetraphosphorus cage). The authors believe that the tetraphosphorus cage was formed by condensation of two units of $[^t\text{Bu(H)N}(^t\text{BuNP})_2\text{N(Li)}^t\text{Bu}]$, followed by the elimination of $^t\text{Bu(H)NLi}$.

In the solid state the heterocubic $[(^t\text{BuNP})_2(^t\text{BuNLi})_2]$ (**10**) is present as a cofacial dimer, the two amido-nitrogens of one heterocube serving as donor atoms towards the lithium atoms of another. A view of this C_2-symmetric molecule (Fig. 7) shows that dimerization is accompanied by the opening of the intracube lithium–amide bonds, leaving all lithium atoms three-coordinate and without a formal electron octet.

All twelve Li–N bonds in **10** fall into the relatively broad range 1.99–2.24 Å, but the disorder and the accompanying uncertainties in the bond lengths do not allow a detailed discussion of these bonds.

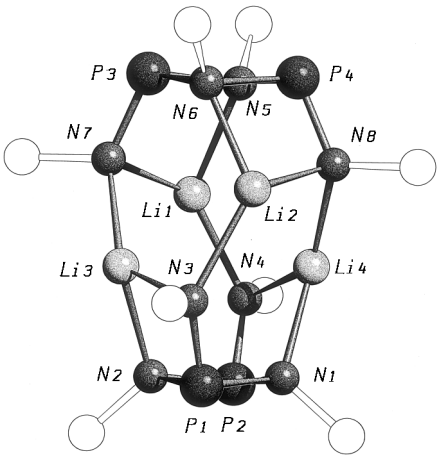

Fig. 7. Solid-state structure of $[(^t\text{BuNP})_2(^t\text{BuNLi})_2]_2$ (**10**). Only the quaternary carbon atoms of the *tert*-butyl groups are shown.

The structure of the dimer is reminiscent of that of the isoelectronic dilithio bis(*tert*-butylamido)cyclodisilazane heterocube [(^{t}BuNSiMe)$_2$(^{t}BuNLi)$_2$] [41]. This silicon analogue forms loose 'dimers' in the solid state, but in contrast to **10** the closest intermolecular distances are between the lithium atoms of one heterocube and the *tert*-butyl hydrogen atoms of another.

An unusual trilithio cage complex [(^{t}BuNPN^{t}Bu)Li]$_3$ (**11**) was isolated as the only product after a 24 h reflux of **1** with two equivalents of ^{n}BuLi in hexanes [42]. This species consists formally of one moiety of the heterocubic [(^{t}BuNP)$_2$(^{t}BuNLi)$_2$] and one moiety of the 1,3-diaza-2-phosphaallyl lithium salt [(^{t}BuNPN^{t}Bu)Li]. Disorder and the ensuing crystallographic problems render a detailed discussion of the bond parameters useless, but the atomic connectivity in this molecule is firmly established.

Structures **10** and **11** are related, because they are the formal tetramers and trimers of [(^{t}BuNPN^{t}Bu)Li], respectively. While the existence of **10** does not prove that species like [(^{t}BuNPN^{t}Bu)Li] are present in solution, the isolation of **11** strongly suggests it. Lithium 1,3-diaza-2-phosphaallyls have been isolated and structurally characterized [43,44], making this a plausible mechanism.

Thus, at least in some cases, deprotonation of the amino groups is either accompanied or followed by ring opening, depending upon experimental conditions. The isolation of a variety of products from the comparatively simple interaction of bis(amino)cyclodiphosph(III)azanes with the strong base ^{n}BuLi shows that these reactions need further study.

5.3. Bis(amido)cyclodiphosph(III)azane compounds of Group 2 elements

5.3.1. Magnesium compounds

Only one bis(amido)cyclodiphosph(III)azane compound of a Group 2 metal, namely [(^{t}BuNP)$_2$(^{t}BuN)$_2$Mg·(THF)$_2$] (**12**), exists [23b]. In contrast to the relatively fast deprotonation of the bis(amino)cyclodiphosph(III)azanes with alkyllithium reagents, the identical reaction with (^{n}Bu)Mg(^{s}Bu) required a 24 h reflux (Eq. (12)). This sluggishness is surprising, and it may be the result of the greater covalence of the magnesium–alkyl bonds and/or of steric hindrance.

The perspective view of **12** in Fig. 8 emphasizes the planarity of the cyclodiphosph(III)azane ring and the coordination geometry of the magnesium atom. This *seco*-heterocube has approximate C_s symmetry and is of structure type **II**. The cyclodiphosph(III)azane moiety functions as a trihapto ligand towards the magnesium atom, forming two covalent Mg–N bonds (2.060(4) Å) and a longer N–Mg donor bond (2.330(4) Å). Two molecules of THF complete the φ-trigonal-bipyramidal ligand arrangement about the metal atom.

5.4. Bis(amido)cyclodiphosph(III)azane cage compounds of Group 13 elements

5.4.1. Boron compounds

Despite the abundance of boron amide species, only one bis(amido)cyclodiphosph(III)azane compound of boron, namely [(^{t}BuNP)$_2$(^{t}BuN)$_2$BPh] (**13**), has been

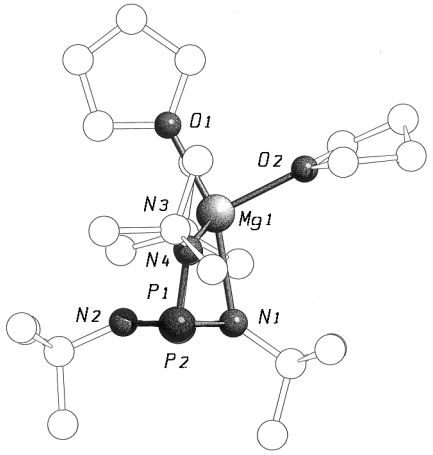

Fig. 8. Solid-state structure of $[(^t\text{BuNP})_2(^t\text{BuN})_2\text{Mg}\cdot(\text{THF})_2]$ (**12**).

reported [37]. Even this molecule, synthesized from $[(^t\text{BuNP})_2(^t\text{BuN})_2\text{SnMe}_2]$ and $PhBCl_2$ as shown in Eq. (13), was not isolated in a pure form. This reaction presumably yields initially $[(^t\text{BuNP})_2(^t\text{BuN})_2\text{SnMeCl}]$ and finally $[(^t\text{BuNP})_2(^t\text{BuN})_2\text{BPh}]$.

Compound **13** was characterized by NMR techniques only, and although these data are consistent with the structure depicted in Scheme 7, a definitive identification must await an X-ray structural analysis. Two singlets at 1.25 and 1.27 δ were the only ligand signals in the ^{1}H-NMR spectrum, while the ^{11}B and ^{31}P spectra showed one singlet each at 35.4 and 178.6 δ, respectively.

The structure of this boron derivative should be similar to that of the gallium compound **15**, shown below, but the small boron atom is unlikely to form a donor bond with the ring-nitrogen atoms.

5.4.2. Aluminum compounds

Because of the critical role of aluminum compounds in polyolefin catalysis, there has been a growing interest in the coordination chemistry of this metal [45,46]. While methylaluminoxane and alkylaluminum species are important cocatalysts in olefin polymerization [47], amido compounds of aluminum are single-component catalysts for this reaction [48].

Recently, for example, cationic aluminum diamidinates were reported to efficiently polymerize ethylene to high molecular-weight polyethylene [48,49]. Bis(amido)cyclodiphosph(III)azanes are related to amidinates, but offer an even more tunable coordination environment for the metal center.

The first bis(amido)cyclodiphosph(III)azane complex of aluminum, $[(Me_3SiNP)_2(Me_3SiN)_2AlCl_2]^-$ (**14**), was reported by Burford and LeBlanc (Eq. (14)). This aluminate was the product of a condensation reaction between two molecules of a zwitterionic diazaphosphoniaaluminatacyclobutane [50].

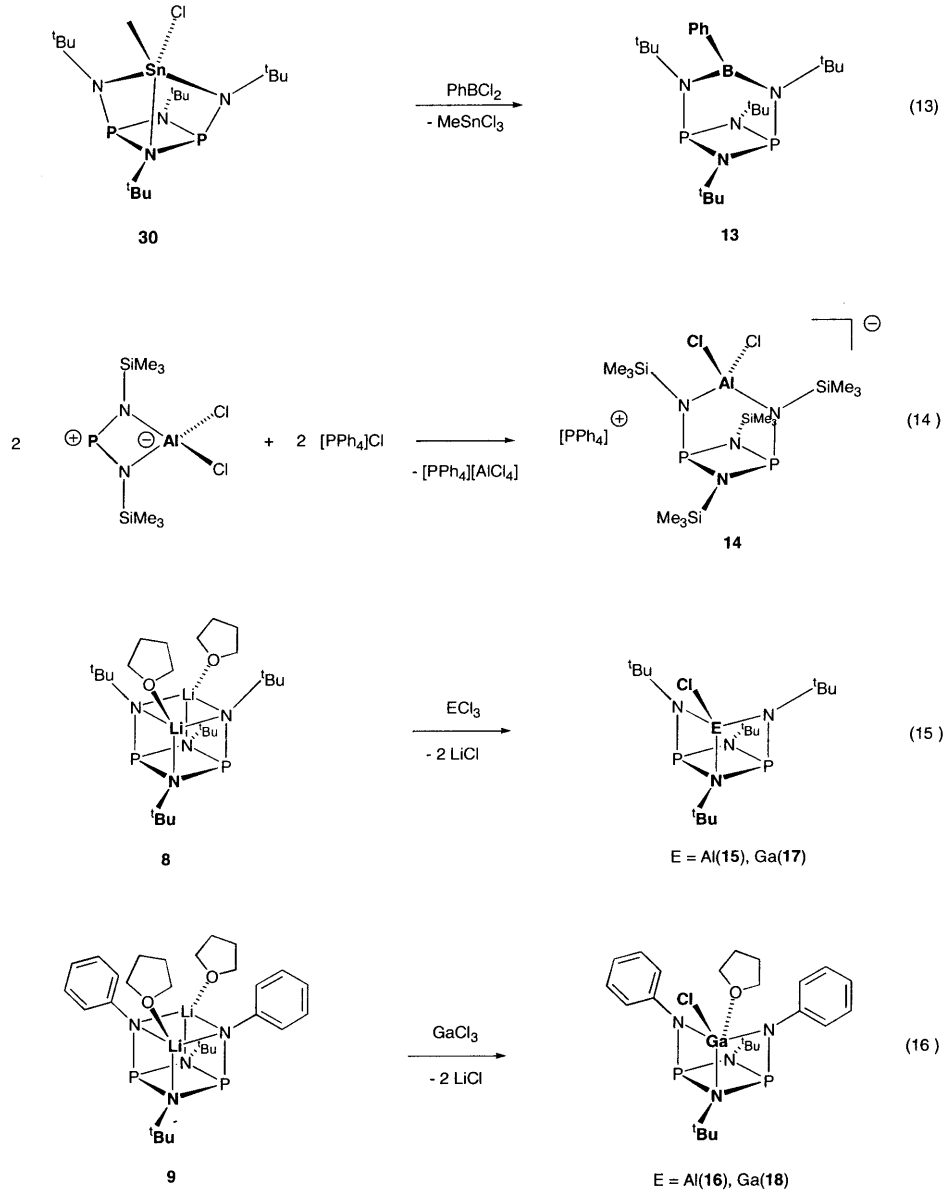

Scheme 7.

Fig. 9 shows a view of the solid-state structure of this almost perfectly C_{2v}-symmetric anion, in which the central aluminum atom is coordinated by one 1,3-bis(trimethylsilyl)-2,4-bis(trimethylsilylamido)cyclodiphosph(III)azane and two chloride ligands. Symmetrical Al–Cl (2.1733(10) Å) and Al–N bonds (1.857(2) Å) and N–Al–N, N–Al–Cl and Cl–Al–Cl bond angles, which range from 106.69(5) to

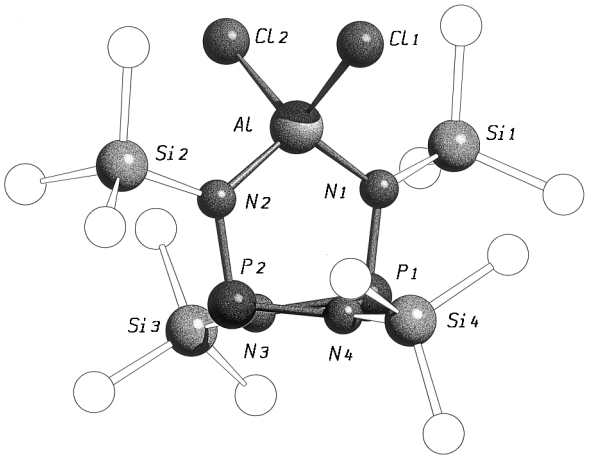

Fig. 9. Solid-state structure of $[(Me_3SiNP)_2(Me_3SiN)_2AlCl_2]^-$ (**14**).

112.69(11)°, define an almost perfectly tetrahedral coordination environment about the aluminum atom. Although the cyclodiphosph(III)azane ring is slightly distorted, its trimethylsilyl-substituents lie approximately in the plane of the ring.

The isolation of this product is significant, because it suggests that the [2 + 2] cycloaddition of two amino(imino)phosphines in the coordination sphere of a metal or metalloid is a mechanism for bis(amido)cyclodiphosph(III)azane formation. The first bis(amido)cyclodiphosph(III)azane compound, namely the antimony species **42** (vide infra) [20], was presumably formed by a similar dimerization of amino(imino)phosphines. Such dimerizations are not the method of choice, however, because bis(amino)cyclodiphosph(III)azanes are easier to synthesize than the amino(imino)phosphines from which they are formed. For symmetrically trimethylsilyl-substituted cyclodiphosph(III)azane ligands, however, this is the only viable route, because trimethylsilylamine is not a stable compound.

By contrast, the neutral aluminum compound $[(^t BuNP)_2(^t BuN)_2AlCl]$ (**15**) was obtained from $[(^t BuNP)_2(^t BuNLi{\cdot}THF)_2]$ and $AlCl_3$ (Eq. (15)) in high yields [51]. In a similar fashion, the reaction of the symmetrically-heterosubstituted $[(^t BuNP)_2(PhNLi{\cdot}THF)_2]$ with $AlCl_3$ gave the analogous $[(^t BuNP)_2(PhN)_2AlCl{\cdot}THF]$ (**16**). It is revealing that the bis(anilido)cyclodiphosph(III)azane species was isolated as a THF complex only, while the bis(*tert*-butylamido)cyclodiphosph(III)azane is solvent free. The presence of the coordinated molecule of THF in **16**, which is valence-isoelectronic with the aluminate **14**, likely reflects the lesser steric bulk of the phenyl-substituted ligand.

Although X-ray data are not yet available for either one of these neutral aluminum compounds, NMR-spectroscopic data suggest that they have the same structure as the gallium analogues **17** and **18**, shown below.

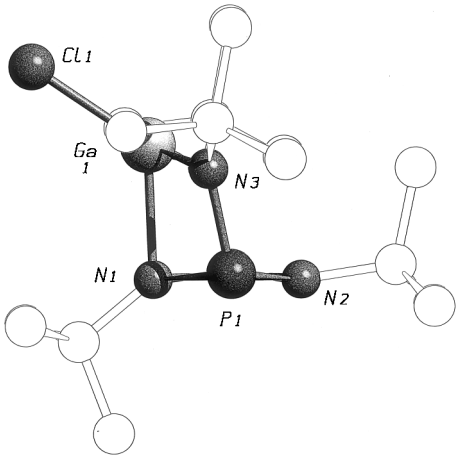

Fig. 10. Solid-state structure of [(^{t}BuNP)$_2$(^{t}BuN)$_2$GaCl] (**17**).

5.4.3. Gallium compounds

Gallium trichloride reacts with one equivalent of **8** in toluene/THF, as shown in Eq. (15), to produce the light-yellow [(^{t}BuNP)$_2$(^{t}BuN)$_2$GaCl] (**17**) [36]. Despite its larger metal center, this compound is free of THF, just like its aluminum analogue (**15**). The identical reaction with [(^{t}BuNP)$_2$(PhNLi·THF)$_2$], in turn (Eq. (16)), afforded the THF adduct [(^{t}BuNP)$_2$(PhN)$_2$GaCl·THF] (**18**) [36], proving that aluminum and gallium have a strictly parallel chemistry with these ligands.

A view of the solid-state structure of **17** (Fig. 10) shows the crystallographic *m* symmetry of this monochloro compound, whose central gallium atom displays a rather unsymmetrical $3+1$ coordination geometry. The gallium–amide bonds (1.886(3) Å) are shorter than the imino-nitrogen–gallium donor bond (2.089(3) Å), but the difference between these two types of bond is the smallest of any compound of this ligand. The former value indicates a typical, albeit slightly shortened, covalent Ga–N bond, while the N–Ga donor bond is somewhat longer than the sum of the covalent radii (2.01 Å). The bond fluxionality exhibited by this tricycle shows that despite its comparative shortness, the N–Ga donor interaction is still a rather weak bond.

An unusual compound, namely the mixed-ligand complex [(^{t}BuNP)$_2$(^{t}BuN)$_2$Ga(^{t}BuNPN^{t}Bu)] (**19**), was obtained from the interaction of **17** with a second equivalent of **8** at slightly elevated temperatures, as shown in Eq. (17) of Scheme 8 [36]. In addition to the bis(amido)cyclodiphosph(III)azane ligand the gallium atom is coordinated by a diazaphosphaallyl moiety (^{t}BuNPN^{t}Bu). Although the source of this heteroallyl has not been firmly established — it could be derived from the dilithio compound [(^{t}BuNP)$_2$(^{t}BuNLi·THF)$_2$] or the ring-opening of coordinated ligand — the former scenario is much more likely.

In a similar reaction (Eq. (17)), designed to definitively establish the source of the heteroallylic moiety, the gallium monochloride complex **18** reacted with one equivalent of [(^{t}BuNP)$_2$(^{t}BuNLi·THF)$_2$] to form [(^{t}BuNP)$_2$(PhN)$_2$Ga(^{t}BuNPN^{t}Bu)] (**20**)

and not [(^{t}BuNP)$_2$(PhN)$_2$Ga(PhNPNPh)] [36]. The solid-state structure of **20** is not known, but analytical and spectroscopic data indicate that at least in solution it is analogous to that of **19**.

While ^{31}P-NMR spectroscopy is not, in general, a good structural tool for bis(amido)cyclodiphosph(III)azane compounds, it is very useful for compounds of these heteroallylic ligands. Their chemical shifts (up to 250 ppm downfield of those of cyclodiphosph(III)azanes) are diagnostic for neutral two-coordinate phosphorus species and are good indicators that the ligand has undergone a cycloreversion.

The formation of the heteroallylic moiety (^{t}BuNPN^{t}Bu) in these reactions is reminiscent of the trilithio complex **11**. The lithium heteroallyl was formed at much higher temperatures, however, suggesting that the ring-opening of [(^{t}BuNP)$_2$(^{t}BuNLi·THF)$_2$] may be catalyzed by the Lewis-acidic [(^{t}BuNP)$_2$(^{t}BuN)$_2$GaCl].

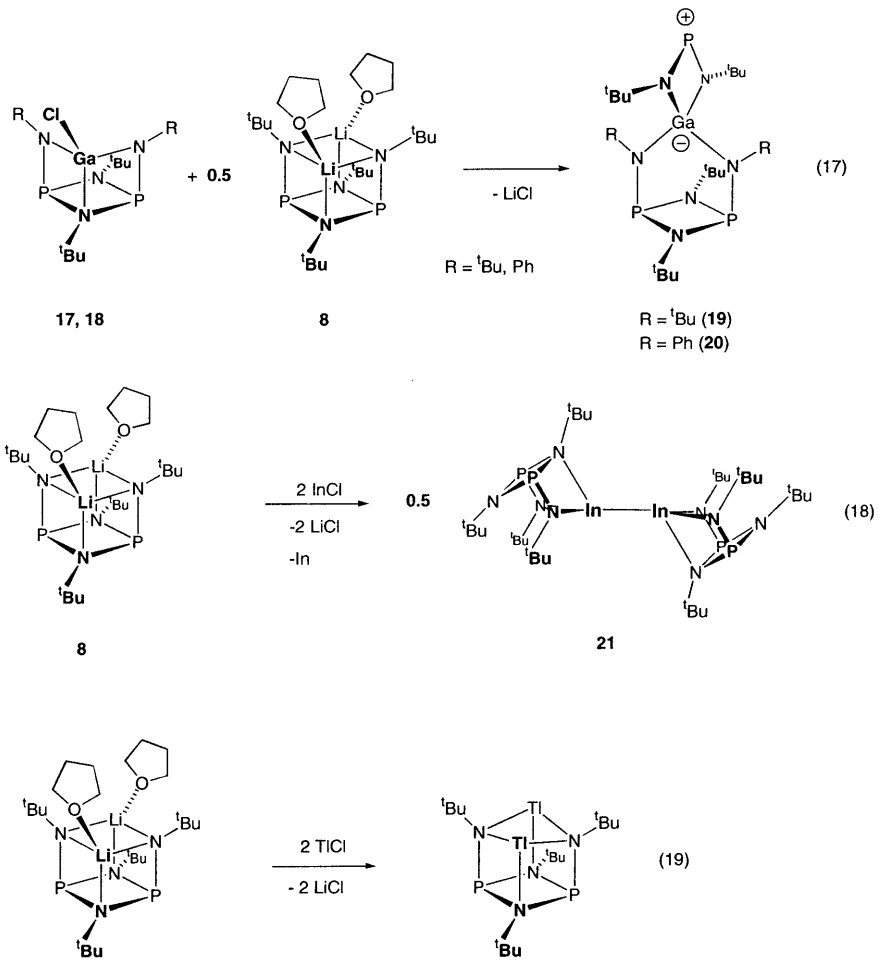

Scheme 8.

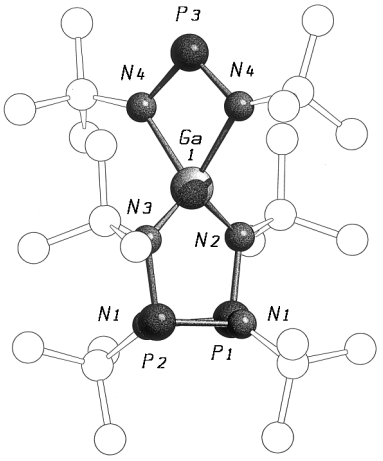

Fig. 11. Solid-state structure of [(^{t}BuNP)$_2$(^{t}BuN)$_2$Ga(^{t}BuNPN^{t}Bu)] (**19**).

Fig. 11 shows a view of the mixed-ligand complex **19**. The molecule has crystallographic *m* symmetry, the mirror plane passing through the gallium and all three phosphorus atoms. Four nitrogen atoms, two from the bis(amido) cyclodiphosph(III)azane and two from the diazaphosphaallyl ligand, coordinate the gallium atom tetrahedrally. The Ga–N bonds to the diazaphosphaallyl nitrogens (2.021(3) Å) are significantly longer than those to the cyclodiphosph(III)azane ligand (1.924(3) and 1.896(3) Å).

It is instructive to contrast the formation of the gallium compounds **19** and **20** with that of the dichloroaluminate **14** [50]. While the cyclodiphosph(III)azane ligand of **14** is the [2 + 2] cycloaddition product of two diazaphosphaallyl moieties, the heteroallylic ligands of the gallium compounds **19** and **20** were formed by the ring opening of bis(amido)cyclodiphosph(III)azanes, i.e. the reverse reaction.

5.4.4. Indium compounds

Neither indium(I) nor indium(III) compounds of bis(amido)cyclodiphosph(III)azane exist, but an indium(II) dimer, with an unsupported, indium–indium bond has been reported [52]. The dimer [(^{t}BuNP)$_2$(^{t}BuN)$_2$In]$_2$ (**21**) was formed by the interaction of indium monochloride with [(^{t}BuNP)$_2$(^{t}BuNLi·THF)$_2$], as shown in Eq. (18).

The isolation of this indium(II) species shows that the indium(I) reactant must have undergone a redox disproportionation during the reaction. The yellow product is surprisingly stable in the solid state, but it slowly decomposes in solution with the formation of a gray precipitate, presumably metallic indium. The diindium compound **21** is isostructural with an indium bis(amido)cyclodisilazane complex synthesized previously [53], proving once again that these two isoelectronic ligands have a parallel coordination chemistry.

Fig. 12 shows a view of the solid-state structure of the C_{2n}-symmetric **21**, whose most unusual feature is the unsupported indium–indium bond. Remarkably, both

indium atoms and the four amido-nitrogen atoms define a perfect plane. The coordination geometry of the metal atoms can therefore be best described as trigonal-planar with a weak intramolecular donor interaction, quite similar to the bonding in the gallium species **17**. The short indium–amide (2.131(2) and 2.140(3) Å) and indium–indium bonds (2.7720(4) Å) presumably reflect the metal atom's low coordination number.

5.4.5. Thallium compounds

In contrast to the nonexistent indium(I) bis(*tert*-butylamido)cyclodiphosph(III)azane, a dithallium derivative $[(^t\text{BuNP})_2(^t\text{BuNTl})_2]$ (**22**) was synthesized straightforwardly from thallium monochloride and **8**, as shown in Eq. (19) [52]. One of the most remarkable chemical properties of **22** is its extreme air-sensitivity, which is impressively demonstrated by the instant blackening of the lemon–yellow complex, even in the solid state.

The ^{31}P-NMR spectrum confirmed the heterocubic structure (type **I**) of this compound, because the phosphorus signal at 111 δ appeared as a broad triplet. Only the coupling of the phosphorus atoms with two equivalent thallium atoms ($I = 0.5$) can account for this splitting pattern.

A view of the solid-state structure of this molecule, which emphasizes the coordination environment of the metal atoms, is shown in Fig. 13. The bimetallic compound is a true heterocube, in which the open corners of the bis(amido)cyclodiphosph(III)azane ligand are occupied by the two very large thallium atoms. As a result of their disproportionately large size, the thallium atoms are highly pyramidalized, with an angle strain (ca. 202°) that can only be borne by such large atoms.

The thallium–nitrogen bonds of the $(\text{Tl–N})_2$ ring are very symmetrical and range from 2.559(3) to 2.587(3) Å, while the donor bonds to the $(\text{P–N})_2$ ring (Tl1–N1 and Tl2–N2) are somewhat longer at 2.613(3) and 2.622(3) Å, respectively. Both sets of bonds are significantly longer than the sum of the covalent radii of these two

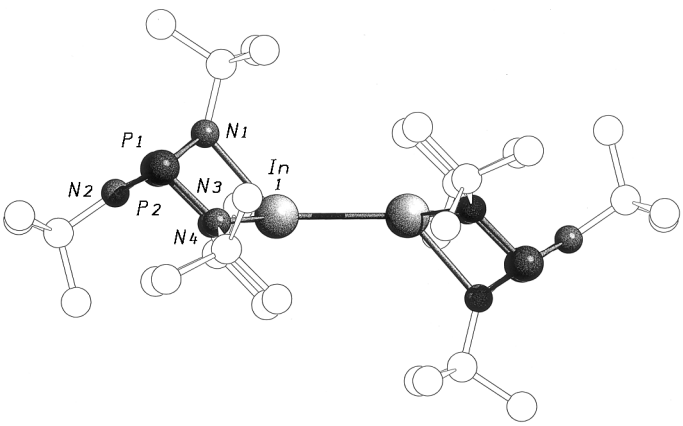

Fig. 12. Solid-state structure of $[(^t\text{BuNP})_2(^t\text{BuN})_2\text{In}]_2$ (**21**).

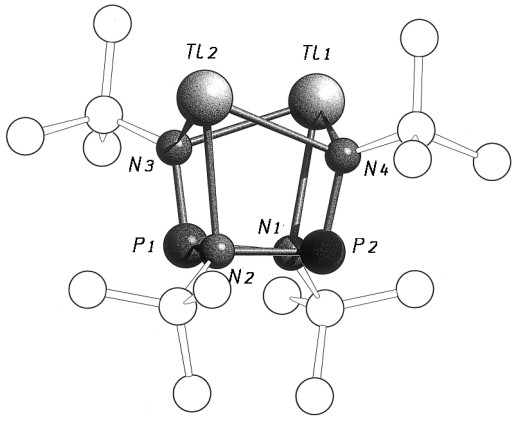

Fig. 13. Solid-state structure of $[(^t\text{BuNP})_2(^t\text{BuNTl})_2]$ (**22**).

elements (2.23 Å), suggesting that the bond lengthening is due to the severe steric crowding of the metal atoms in this cube. The intra-cube thallium–thallium separation is only 3.5462(3) Å, cf. $r_{cov}(\text{Tl}) = 1.48$ Å.

Just as for the indium species **21**, an isoelectronic cyclodisilazane compound of **22** exists [41]; and just as for **21**, its bond parameters are virtually identical to those of the cyclodisilazane analogue. In addition to being isostructural with the cyclodisilazane derivative, the dithallium compound **22** is structurally related to the lithium salts **8** and **10**.

It is instructive to contrast the solid-state structures of these three compounds. In $[(^t\text{BuNP})_2(^t\text{BuNLi}\cdot\text{THF})_2]$ each lithium atoms achieves an octet by the electron-pair donation from the THF molecules, while in **22** the thallium atoms have an electron octet, and require neither the presence of solvent molecules, nor the electron-donation from another molecule. In the dimer **10**, by contrast, the lithium atoms are formally electron deficient, having only six electrons each.

5.4.6. Molecular fluxionality of Group 13 compounds

With the exception of the dithallium complex **22** and the mixed-ligand gallium species **19** and **20**, all cyclodiphosph(III)azane compounds of Group 13 elements are C_s-symmetric. This statement implies that the *tert*-butylimino groups are diastereotopic and should appear as two distinct signals in the ^{1}H-NMR spectra. Room-temperature, and even low-temperature, ^{1}H-NMR spectra of most Group 13 bis(amido)cyclodiphosph(III)azane compounds, except those containing THF, however, exhibit only one singlet for these substituents.

These observations can be explained in terms of a fluxional interaction of the Group 13 element with the ring-nitrogen atoms. Because the ground state structures cannot be frozen out, even at -100°C, the activation energies for this process must be very low, and possibly less than 32 kJ mol^{-1}. These low activation energies, in turn, confirm that the donor bonds between Group 13 element and imino-nitrogens are weak.

5.5. Bis(amido)cyclodiphosph(III)azane cage compounds of Group 14 elements

5.5.1. Carbon compounds

A bis(amino)cyclodiphosph(III)azanes in which the amino nitrogen atoms are connected by an ethylene bridge is the only bicyclic carbon derivative of this ligand.

This carbon–nitrogen–phosphorus heterobicycle, $[(^t\mathrm{BuNP})_2(^t\mathrm{BuNCH}_2)_2]$ (**23**), was prepared in modest yields of 10% from the dichloro derivative **4** according to Eq. (20) of Scheme 9 and was characterized by analytical and spectroscopic techniques only [54]. These data and an X-ray study of an isoelectronic compound with a $O(CH_2)_3O$ link (reported in the same article), however, strongly suggest that **23** has a structure like that of the diphosphine species **40**, shown below. Similar bicyclic compounds are also known for cyclodiphosph(V)azanes and mixed cyclodiphosph(III/V)azanes [55].

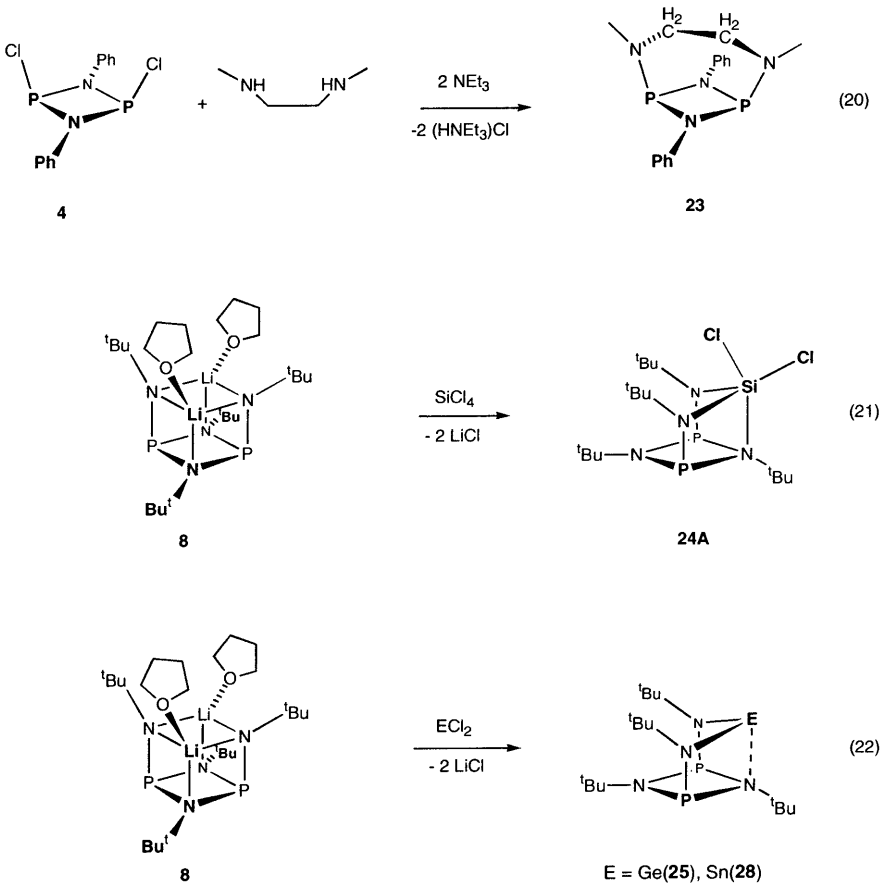

Scheme 9.

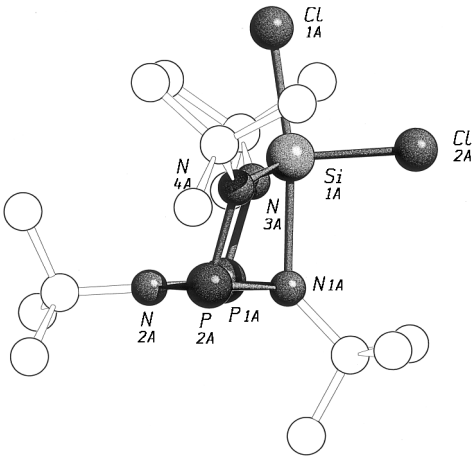

Fig. 14. Solid-state structure of $[(^t\text{BuNP})_2(^t\text{BuN})_2SiCl_2]$ (**24A**).

5.5.2. Silicon compounds

The slow addition of $[(^t\text{BuNP})_2(^t\text{BuNLi}\cdot\text{THF})_2]$ to a toluene solution of $SiCl_4$ (Eq. (21)) afforded $[(^t\text{BuNP})_2(^t\text{BuN})_2SiCl_2]$ (**24**) in high yields of over 87% [56]. This silicon compound exhibits only two singlets in its ^{1}H-NMR spectrum, indicative of either a symmetric structure of type **III** or a fluxional one of type **II**.

There are two crystallographically-independent molecules in the monoclinic unit cell, both of which have approximate C_s symmetry. The presence of both isomers in the solid state shows that their conformations must be close in energy. With the exception of the N–Si donor bonds, the bond lengths for both isomers are almost identical, as shown in Table 2.

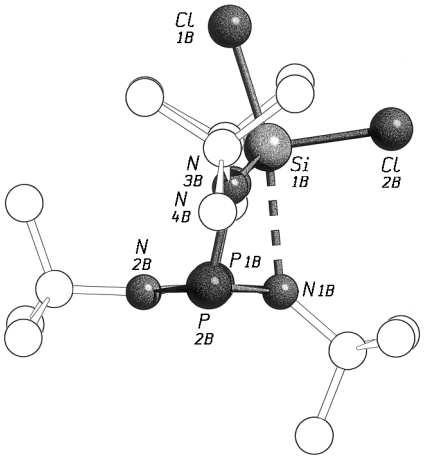

Fig. 15. Solid-state structure of $[(^t\text{BuNP})_2(^t\text{BuN})_2SiCl_2]$ (**24B**).

Table 2
Selected bond lengths (in Å) for bis(amido)cyclodiphosph(III)azane compounds mentioned in the text

Compound	P–λ^3N *endo* (mean)	P–λ^4N *endo* (mean)	P–N *exo* (mean)	E–N (mean)	E–N donor (mean)	E–X (mean)
$[(^t\text{BuNP})_2(^t\text{BuNLi}\cdot\text{THF})_2]$ (**8**)	–	1.778(2)	1.651(2)	2.086(5)	2.112(5)	1.957(5)
$[(^t\text{BuNP})_2(\text{PhNLi}\cdot\text{THF})_2]$ (**9**)	–	1.763(3)	1.678(3)	2.076(6)	2.094(6)	1.870(6)
$[(^t\text{BuNP})_2(^t\text{BuNLi})_2]_2$ (**10**)	–	1.779(10)	1.650(9)	2.04(3)	2.17(3)	2.06(3)
$[(^t\text{BuNP})_2(^t\text{BuN})_2\text{Mg(THF)}_2]$ (**12**)	1.754(4)	1.780(4)	1.656(4)	2.060(4)	2.330(4)	2.082(4)
$[(\text{Me}_3\text{SiNP})_2(\text{Me}_3\text{SiN})_2\text{AlCl}_2]^-$ (**14**)	1.731(2)	–	1.677(2)	1.857(2)	–	2.1733(10)
$[(^t\text{BuNP})_2(^t\text{BuN})_2\text{GaCl}]$ (**17**)	1.727(2)	1.808(2)	1.692(2)	1.886(2)	2.089(3)	2.1600(9)
$[(^t\text{BuNP})_2(^t\text{BuN})_2\text{Ga(NPN)}]$ (**19**) (NPN = ^{t}BuNPN^{t}Bu)	1.728(3)	–	1.694(4)	1.910(3)	–	2.021(3)
$[(^t\text{BuNP})_2(^t\text{BuN})_2\text{In}]_2$ (**21**)	1.724(3)	1.808(3)	1.671(3)	2.135(2)	2.315(2)	2.7720(4), In–In
$[(^t\text{BuNP})_2(^t\text{BuNTl})_2]$ (**22**)	–	1.773(3)	1.659(3)	2.570(3)	2.618(3)	–
$[(^t\text{BuNP})_2(^t\text{BuN})_2\text{SiCl}_2]$ (**24A**)	1.715(3)	1.750(3)	1.716(3)	1.742(3)	–	2.084(1)
$[(^t\text{BuNP})_2(^t\text{BuN})_2\text{SiCl}_2]$ (**24B**)	1.716(3)	1.770(3)	1.705(3)	1.752(3)	2.168(3)	2.108(1)
$[(^t\text{BuNP})_2(^t\text{BuN})_2\text{SnMe}_2]$ (**29**)	1.741(8)	–	1.678(9)	2.076(9)	2.762(9)	Not given
$[(^t\text{BuNP})_2(^t\text{BuN})_2\text{SnMeCl}]$ (**30**)	1.70(1)	1.76(1)	1.70(1)	2.06(1)	2.45(1)	Not given
$[(^t\text{BuNP})_2(^t\text{BuN})_2\text{SnCl}_2]$ (**31**)	1.722(5)	1.773(4)	1.689(5)	2.050(5)	2.454(4)	2.347(2)
$[(^t\text{BuNP})_2(^t\text{BuN})_2\text{SnO}]_2$ (**32**)	1.728(2)	1.788(2)	1.690(2)	2.070(2)	2.327(3)	1.997(3), 2.014(3)
$[(^t\text{BuNP})_2(^t\text{BuN})_2\text{SnS}]_2$ (**33**)	1.726(2)	1.791(2)	1.691(3)	2.084(3)	2.403(4)	2.4157(12), 2.4601(12)
$[(^t\text{BuNP})_2(^t\text{BuN})_2\text{SnSe}]_2$ (**34**)	1.723(3)	1.787(3)	1.697(3)	2.075(3)	2.420(4)	2.5420(6), 2.5980(6)
$\{[\text{SP}(^t\text{BuN})_2\text{P}](^t\text{BuN})_2\text{SnS}\}_2$ (**35**)	1.702(3)	1.746(4)	1.667(3)	2.096(3)	2.539(3)	2.4146(10), 2.4542(10)
$[(^t\text{BuNP})_2(^t\text{BuN})_2\text{PCl}]$ (**37**)	1.720(4)	–	1.733(4)	1.689(4)	–	2.244(3)
$[(^t\text{BuNP})_2(^t\text{BuN})_2\text{PN}_3]$ (**38**)	1.715(2)	–	1.740(4)	1.696(3)	–	1.852(4)
$[(^t\text{BuNP})_2(^t\text{BuNPPh})_2]$ (**40**)	1.734(2)	–	1.739(2)	1.730(2)	–	P–P bond, 2.175(1)
$[(^t\text{BuNP})_2(^t\text{BuN})_2\text{AsCl}]$ (**41**)	1.718(2)	–	1.727(2)	1.843(2)	–	2.3325(11)
$[(^t\text{BuNP})_2(^t\text{BuN})_2\text{SbCl}]$ (**42**)	1.719(4)	1.772(5)	1.680(6)	2.095(5)	2.413(5)	2.492(3)
$[(^t\text{BuNP})_2(\text{PhN})_2\text{SbCl}]$ (**43**)	1.717(2)	1.774(2)	1.699(2)	2.088(2)	2.490(2)	2.439(1)
$[(^t\text{BuNP})_2(^t\text{BuN})_2\text{SbN}_3]$ (**44**)	1.719(4)	1.778(4)	1.681(4)	2.073(4)	2.421(4)	2.199(4)
$[(^t\text{BuNP})_2(^t\text{BuN})_2\text{SbOPh}]$ (**45**)	1.722(8)	1.756(8)	1.681(8)	2.092(8)	2.472(8)	2.031(8)
$[(^t\text{BuNP})_2(^t\text{BuN})_2\text{Sb(HMDS)}]$ (**46**) (HMDS = $\text{N(SiMe}_3)_2$)	1.729(3)	1.751(3)	1.685(3)	2.122(2)	2.656(2)	2.099(2)

Molecule **24A** (Fig. 14) has a more pronounced Si–N donor bond 2.168(3) Å than **24B** (2.423(5) Å), whose structure is shown in Fig. 15. Given that a typical Si–N single bond is about 1.75 Å long, both contacts are weak bonds at best. Although the Si–N1 separation in **24A** can still be considered a bond, in **24B** it is drawn as a dashed line only. The covalent silicon–amide bonds are symmetrical and isometric in both molecules, spanning the narrow range 1.739(3)–1.752(3) Å. In contrast to these silicon–amide bonds, the silicon–chloride bonds vary significantly, ranging from 2.1449(13) and 2.0705(13) Å in molecule **24A**, to 2.101(2) and 2.0670(14) Å in molecule **24B**. Notably, the longest Si–Cl bond is *trans* to the shortest N–Si donor bond in both molecules.

5.5.3. Germanium compounds

5.5.3.1. Germanium(II) compounds. The light-yellow divalent germanium compound $[(^t\text{BuNP})_2(^t\text{BuN})_2\text{Ge}]$ (**25**) was synthesized from $GeCl_2$(dioxane) and $[(^t\text{BuNP})_2(^t\text{BuNLi}\cdot\text{THF})_2]$, as shown in Eq. (22) [56]. The molecular composition of **25** was deduced from NMR spectroscopic and analytical techniques, because its solid-state structure is still unknown. The germanium atom in this molecule has an electron sextet and can thus be expected to have a significant interaction with the imino-nitrogens. Both the ^{1}H- and ^{31}P-NMR data are in agreement with a structure of type **II** or **III**. Structure **II**, with a fluxional germanium atom, is the more probable, but its ground state could not be frozen out, due to a very low activation energy for site exchange.

5.5.3.2. Germanium(IV) compounds. In contrast to its silicon analogue, the tetravalent germanium complex $[(^t\text{BuNP})_2(^t\text{BuN})_2\text{GeCl}_2]$ (**26**) was not prepared by the metathesis reaction of $GeCl_4$ with **8**, but was obtained instead by the transmetallation of $[(^t\text{BuNP})_2(^t\text{BuN})_2\text{Sn}]$ with germanium tetrachloride (Eq. (25) [57]. This reaction is driven to completion by the insolubility of $SnCl_2$ in the toluene solvent, but the product was contaminated with small amounts of $[(^t\text{BuNP})_2(^t\text{BuN})_2\text{SnCl}_2]$. The presence of the tin(IV) species (vide infra) shows that this reaction is not a simple exchange, but that it is accompanied by chloride transfer and thus a redox reaction. Successive recrystallizations removed these tin(IV) impurities quantitatively.

The solid-state structure of **26** is not known. Crystal morphology, as well as melting point and ^{1}H- and ^{31}P-NMR spectra, however, suggest that this germanium(IV) compound has a structure similar to those of the silicon (**24**) and tin (**31**) analogues.

As expected, **25** is highly reactive, being instantly oxidized by dioxygen (Eq. (26)) to $[(^t\text{BuNP})_2(^t\text{BuN})_2\text{GeO}]_2$ (**27**) [56]. This colorless dimer, which is much more soluble than its tin analogue **32**, revealed only three singlets in the ^{1}H-NMR spectrum in a 2:1:1 intensity ratio. The peak pattern is typical of a *seco*-heterocubic structure, in which the germanium atom forms a donor bond with an imino-nitrogen atom.

A single-crystal X-ray study confirmed the dimeric nature of **27** in the solid state, but the molecule was disordered on a three-fold axis of the cubic space group *Pa*-3. The molecule is isoelectronic with the cyclodisilazane analogue $[(^t\text{BuNSi})_2(^t\text{BuN})_2\text{GeO}]_2$, however, for which a fully ordered structure was found on refinement [58]. The inspection of the averaged bond parameters for **27** suggested that both compounds are likely isostructural. In the cyclodisilazane compound the unique Ge–O bonds of the central $(\text{Ge–O})_2$ ring are 1.809(4) and 1.825(4) Å, while for **27** these bonds are 1.79(2) and 1.87(2) Å, respectively.

5.5.4. Tin compounds

5.5.4.1. Tin(II) compounds. Tin dichloride reacts with one equivalent of **8**, according to Eq. (22), to furnish the bright-yellow, air-sensitive $[(^t\text{BuNP})_2(^t\text{BuN})_2\text{Sn}]$ (**28**) [57]. Although this tin(II) species was fully characterized by conventional spectroscopic and analytical techniques, X-ray structural studies were frustrated by the plastic nature of the solid. A theoretical investigation of the molecule at the MP2 level predicts a *seco*-heterocubic structure of type **II**, as exhibited its germanium analogue [57].

5.5.4.2. Tin(IV) compounds. Nöth and co-workers attempted the synthesis of $\text{ClP}(\mu\text{-N}^t\text{Bu})_2\text{SnMe}_2$ via the comproportionation of $\text{Cl}(^t\text{BuNP})_2\text{Cl}$ (**3**) and the cyclodistannazane $\text{Me}_2\text{Sn}(\mu\text{-N}^t\text{Bu})_2\text{SnMe}_2$, as shown in Eq. (23), but isolated the tin dimethyl species $[(^t\text{BuNP})_2(^t\text{BuN})_2\text{SnMe}_2]$ (**29**) instead [37]. This tetravalent tin compound was the first fully-characterized metal derivative of a bis(amido)cyclodiphosph(III)azane

A line drawing of the C_s-symmetric molecule is shown in Scheme 10. The metal atom is not centered above the cyclodiphosph(III)azane ring, but displaced slightly towards one of the imino-nitrogen atoms, with an Sn–N separation of 2.762(9) Å. This distance is shorter than the sum of the van der Waals radii of tin and nitrogen, but too long to be considered a true bond. The symmetrical tin–amide bonds, by contrast, have typical lengths of 2.063(9) and 2.086(9) Å.

Treatment of this dimethyltin derivative with dichlorophenylborane (Eq. (24)), in an attempted synthesis of the boron derivative **13**, led to the chloro–methyl–tin compound $[(^t\text{BuNP})_2(^t\text{BuN})_2\text{SnMeCl}]$ (**30**) instead [37]. As expected, compound **30** has a similar structure as the dimethyl analogue **29**, with the notable exception that the separation between imino-nitrogen and tin is now only 2.45(1) Å and thus close enough to be considered a bond. Although the smaller van der Waals radius of chlorine (1.7 Å) versus methyl (2.0 Å) may be responsible for the structural differences in these tin(IV) compounds, the authors think that the increased Lewis-acidity of the tin atom is the principal reason for the shorter donor bond.

The final member of this series of tin(IV) bis(amido)cyclodiphosph(III)azanes, namely $[(^t\text{BuNP})_2(^t\text{BuN})_2\text{SnCl}_2]$ (**31**), was prepared by the interaction of $[(^t\text{BuNP})_2(^t\text{BuN})_2\text{Sn}]$ with SnCl_4 (Eq. (25)). The metathesis of SnCl_4 with **8** failed to give product [56]. From a mechanistic point of view it is interesting to speculate, whether this reaction is merely an oxidation of the chelated tin(II), or a true metal

exchange. The example of the analogous reaction with $[(^tBuNP)_2(^tBuN)_2Ge]$ (vide supra) suggests that both, interchange and redox reactions, occur.

Selected bond lengths for **31** are given in Table 2 and its solid-state structure is shown in Fig. 16. The perspective view emphasizes the near-planarity of the cyclodiphosph(III)azane ring and the φ-tbp coordination environment of the tin atom. The tin–amide bonds are symmetrical (2.044(5) and 2.055(5) Å), but there is a slight asymmetry in the tin–chloride bonds (2.335(2) and 2.358(2) Å). The Sn–N(2) donor bond has the same length (2.453(4) Å) as in the monochloro derivative **30**. Because the dichloro compound **31** can be assumed to have a more Lewis-acidic metal center than **30**, the value of 2.45 Å apparently constitutes the minimal nitrogen to tin donor-bond length in these tin(IV) compounds.

5.5.4.3. Chalcogen-linked seco-heterocubic tin(IV) compounds. Divalent tin is chalcophilic and susceptible to attack by oxygen, sulfur and selenium, but slightly less so than germanium. Exposure of **28** to dioxygen (Eq. (26) of Scheme 11) led to its rapid oxidation and the formation of $[(^tBuNP)_2(^tBuN)_2SnO]_2$ (**32**) as indicated by the immediate appearance of an insoluble precipitate [56]. Oxidation by sulfur and

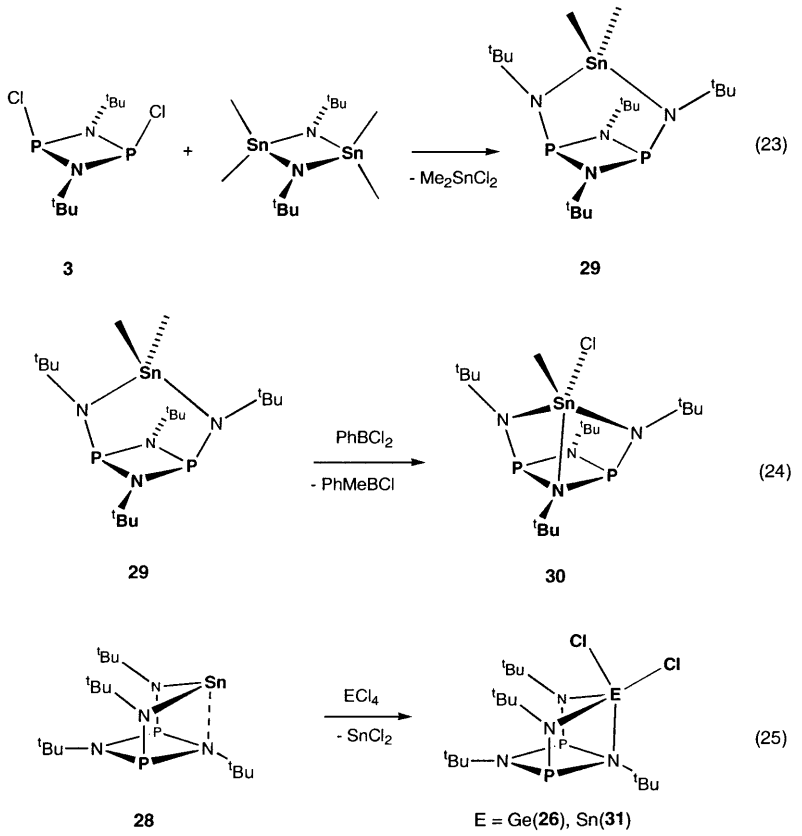

Scheme 10.

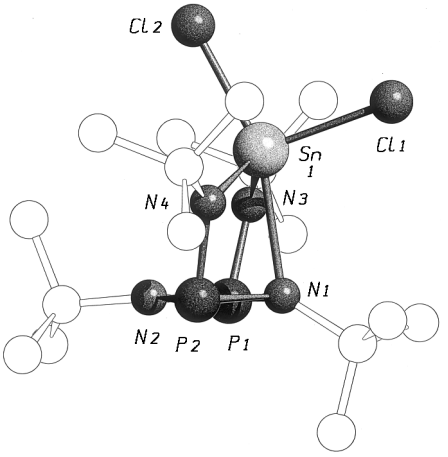

Fig. 16. Solid-state structure of $[(^{t}BuNP)_2(^{t}BuN)_2SnCl_2]$ (**31**).

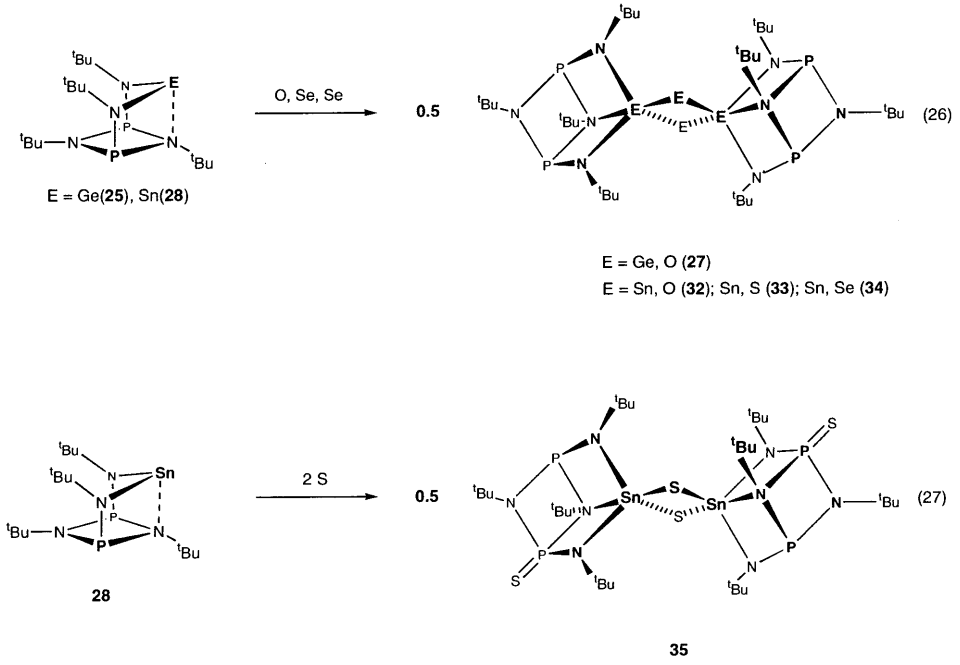

Scheme 11.

selenium was much slower, however, and required elevated temperatures. Upon cooling, similar light-yellow solids of $[(^{t}BuNP)_2(^{t}BuN)_2SnS]_2$ (**33**) and $[(^{t}BuNP)_2(^{t}BuN)_2SnSe]_2$ (**34**) crystallized from these solutions. The extreme insolubility of these solids in all common solvents suggested that they were dimers or oligomers and made structural assignment by NMR techniques impossible.

A conclusive characterization could, therefore, come only from single-crystal X-ray analyses. The three compounds **32**–**34** are isomorphous and crystallize in the monoclinic space group $C2/m$ with site symmetry $2/m$ [57]. The view of the solid-state structure of the oxide dimer **32** in Fig. 17 demonstrates this high molecular symmetry.

An almost square $(Sn–O)_2$ ring with nearly identical Sn–O bonds of 1.997(3) and 2.014(3) Å constitutes the central portion of this centrosymmetric molecule. These relatively short tin–oxygen bonds (sum of covalent radii = 2.14 Å) may reflect the low-coordination number of the oxygen atoms. The bis(amido)cyclodiphosph(III)azane moieties bind the tin atoms in a trihapto fashion, with equidistant tin–amide bonds (2.070(2) Å) and an imino-nitrogen–tin donor bond of 2.327(3) Å length. Remarkably, the cyclodiphosph(III)azane ring is almost completely planar, despite the significant out-of-plane distortion of one of the imino *tert*-butyl groups. The coordination geometry about the tin atom is trigonal bipyramidal, with N1 and O1 forming the axial substituents, and N3, N3' and O2 the slightly distorted equatorial substituents of the metal.

The sulfur and selenium compounds **33** and **34** are isostructural with the oxide dimer, the major differences being the central (Sn–E) rings. In **33** the Sn–S bonds are 2.4157(12) and 2.4601(12) Å, respectively, and thus more asymmetrical than those in **32**. In contrast to the short tin–oxygen bonds, these tin–sulfur bonds match the sum of the covalent radii (2.44 Å) perfectly. Similar bond trends were found for the selenium derivative **34** (Fig. 18).

While tin oxidation in these compounds is much more rapid than ligand oxidation, the ligand can be oxidized on prolonged heating in the presence of excess chalcogen [37]. An example of such a reaction is the oxidation of **28** with excess sulfur (Eq. (27)), which yielded the mixed cyclodiphosph(III/V)azane polycycle $\{[SP(\mu\text{-}^t\text{BuN})_2P](^t\text{BuN})_2SnS\}_2$ (**35**) [57]. Oxidation of coordinated ligand, however, is much slower than oxidation of free ligand [59].

The X-ray crystallographic analysis confirmed the formulation of **35** as that shown above [57]. Fig. 19 shows a view of the truncated solid-state structure of this dimer, which is disordered about an inversion center. The averaging of bonds does not allow a distinction to be made between chemically nonequivalent P–N bonds.

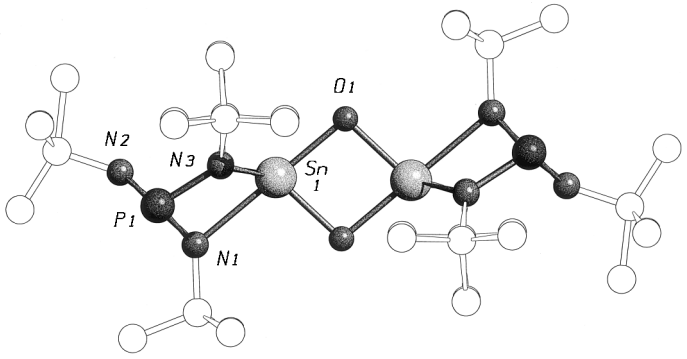

Fig. 17. Solid-state structure of $[(^t\text{BuNP})_2(^t\text{BuN})_2SnO]_2$ (**32**).

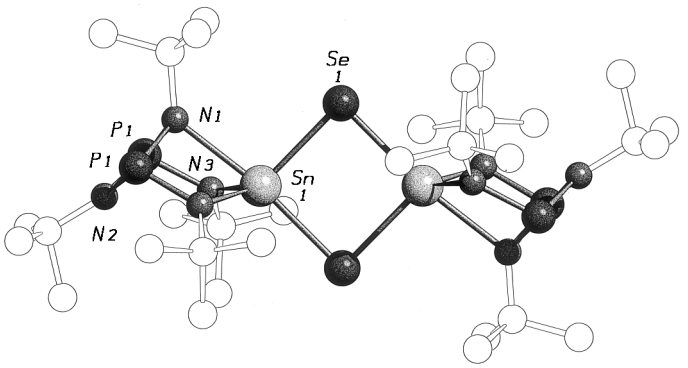

Fig. 18. Solid-state structure of $[(^t\text{BuNP})_2(^t\text{BuN})_2\text{SnSe}]_2$ (**34**).

These averaged P–N bonds are shorter than the corresponding bonds in **32**–**34**, being intermediate between those in cyclodiphosph(III)azanes and cyclodiphosph(V)azanes. The endocyclic P–λ^3N and P–λ^4N bonds of **35**, for example, are 1.703(3) and 1.746(4) Å, while the exocyclic P–N bonds are only 1.667(3) Å. These values may be compared to the corresponding bonds in **33**, which are 1.726(2), 1.791(2) and 1.691(2) Å, respectively.

In notable contrast, the tin–amide bonds are slightly longer in this mixed cyclodiphosph(III/V)azane, while the nitrogen–tin donor bond (2.539(3) Å) is much longer than that in **33**. These bond trends are in good agreement with the expected greater electron-withdrawing properties of the phosphorus(V) center.

The disorder has its most profound effect on the P=S bond, which appears short, being only 1.890(2) and 1.853(3) Å for the major and minor contributor, respectively. These bonds are much shorter, than those in ordered structures of dithiocy

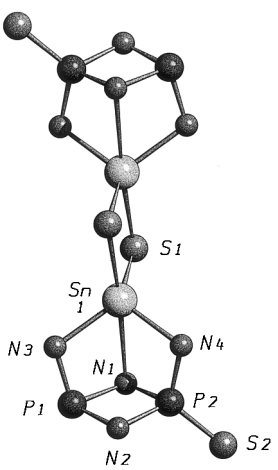

Fig. 19. Solid-state structure of $\{[\text{SP}(\mu\text{-}^t\text{BuN})_2\text{P}](^t\text{BuN})_2\text{SnS}\}_2$ (**35**). Only the polycyclic inorganic framework is shown.

clodiphosph(V)azanes. For the closely related cyclodiphosph(V)azane [^{t}Bu(H)N(^{t}BuNPS)$_2$N(H)^{t}Bu], for example, an average P=S bond length of 1.925(1) Å was found [59].

5.6. Bis(amido)cyclodiphosph(III)azane compounds of Group 15 elements

5.6.1. Phosphorus(III) compounds

The first reported bicyclic phosphorus compound of a bis(amino)cyclodiphosph(III)azane was [(EtNP)$_2$(EtN)$_2$PN(H)Et] (**36**). The heterobicycle was synthesized by the aminolysis of a 1,3,5-triethyl-2,4,6-trichlorocyclotriphosph(III)azane with ethylamine, as shown in Eq. (28) of Scheme 12 [9]. Reference to this compound was made only in a review, however, and thus synthetic and structural details are missing. Two ^{31}P-NMR signals at 97.1 and 106.0 δ, with a 2:1 intensity ratio, were assigned to the ring and central phosphorus atoms, respectively, but no other analytical or spectroscopic data were given.

The simplest conceivable bicyclic phosphorus derivative of a bis(amido)cyclodiphosph(III)azane, namely [(^{t}BuNP)$_2$(^{t}BuN)$_2$PCl] (**37**), was synthesized recently from PCl_3 and **8** in toluene, as shown in Eq. (29) [60]. This compound has structure type **III**, the unique phosphorus atom being located directly above the center of the cyclodiphosph(III)azane ring. Lone pair electrons and the chloride ligand on the unique phosphorus atom render the imino-nitrogen substituents diastereotopic, and this is reflected in two NMR signals that remain separate up to the highest attainable temperatures.

Fig. 20 shows that compound **37** is an inorganic bicycle of alternating phosphorus and nitrogen atoms with crystallographic *m* symmetry. Three of the nitrogens are almost perfectly trigonal planar, but N2 is pyramidalized (349.8°), due to the repulsive interaction of its *tert*-butyl group with the chloride ligand. The three chemically-unique P–N bonds in the ligand portion of this compound range from 1.713(2) to 1.740(4) Å. The P2–N3 bonds are the shortest (1.689(4) Å) phosphorus–nitrogen bonds in this compound, and they may reflect partial double-bond character.

Judging from the puckered cyclodiphosph(III)azane ring, the relatively small phosphorus atom is a poor fit for the large bite of the ligand and causes sufficient strain in the molecule to distort (355.6°) the normally planar ring. Compared to the P–Cl bonds in the dichlorocyclodiphosph(III)azane **3** (2.105(9) Å) [30], the phosphorus–chloride bond in **37** is very long (2.244(3) Å).

Treatment of **37** with sodium azide or lithium hexamethyldisilazide (Eq. (30)) yielded the azido and hexamethyldisilazido compounds [(^{t}BuNP)$_2$(^{t}BuN)$_2$PN$_3$] (**38**) and [(^{t}BuNP)$_2$(^{t}BuN)$_2$PN(SiMe$_3$)$_2$] (**39**), respectively [60]. These are thermally stable, colorless, air-sensitive solids, of which the azide derivative is a potential precursor for the reactive phosphinonitrenes [61].

Only compound **38** was characterized by single-crystal X-ray diffraction and the results of this study are shown in Fig. 21. The view of the molecule emphasizes the perpendicular dispositions of (P–N)$_2$ ring, P1–N3–P2 moiety and azide ligand. With

the exception of the azide ligand, all structural parameters of **38** are identical to those of **37**. The phosphorus–azide bond (1.852(4) Å) is much longer than those in conventional phosphorus–azides (1.74 Å) [62].

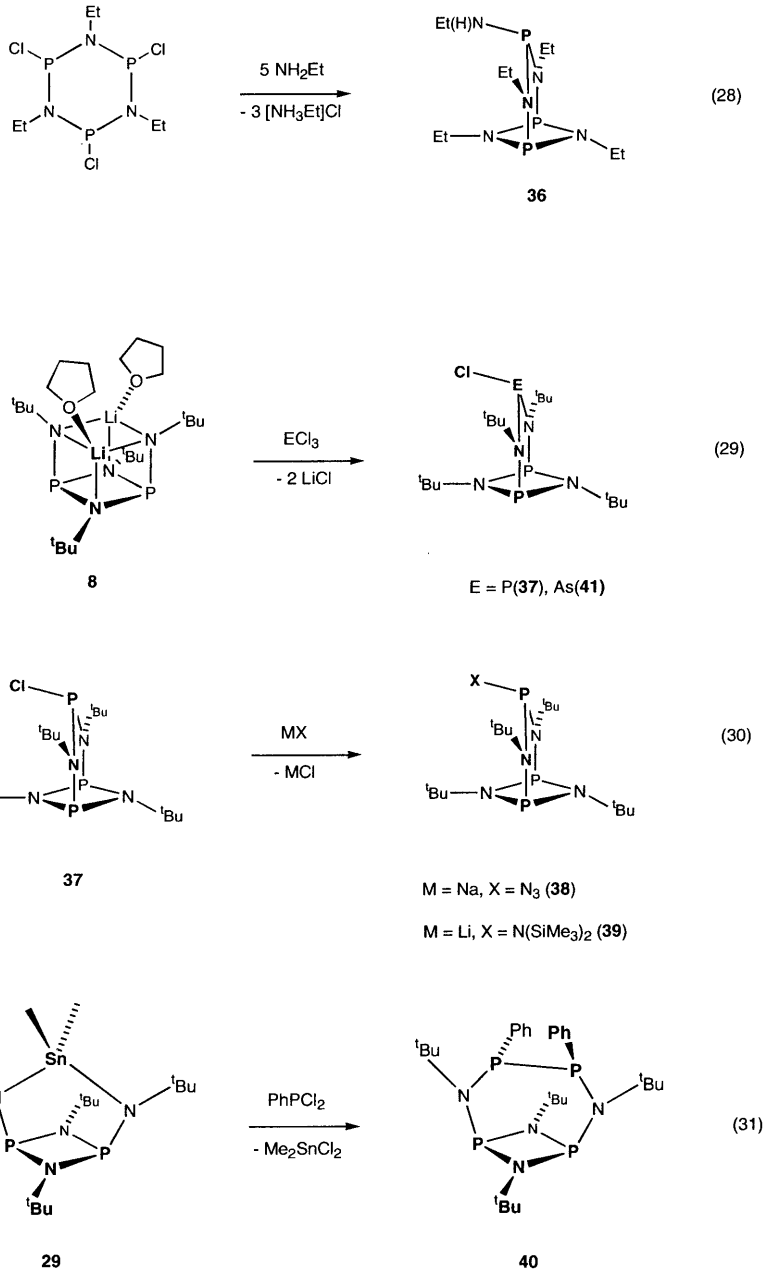

Scheme 12.

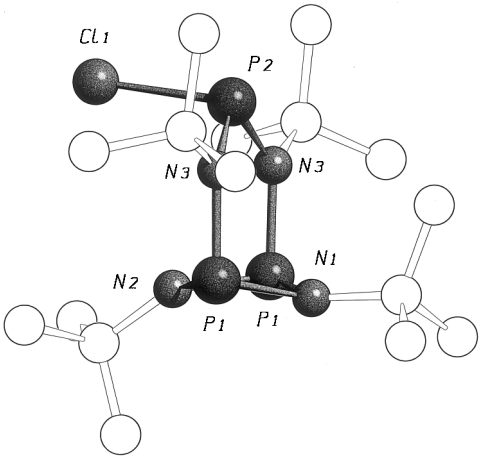

Fig. 20. Solid-state structure of [(^{t}BuNP)$_2$(^{t}BuN)$_2$PCl] (**37**).

Prior to the syntheses of these monophosphorus compounds, an unusual diphosphine compound of the ligand, namely [(^{t}BuNP)$_2$(^{t}BuNPPh)$_2$] (**40**), had been reported [37]. It was produced by the reaction of [(^{t}BuNP)$_2$(^{t}BuN)$_2$SnMe$_2$] with $PhPCl_2$ (Eq. (31)). Obviously, the phenyldichlorophosphine underwent a redox reaction in this exchange, but the oxidation product, possibly $PhPCl_4$, was not isolated. The authors point out that the formation of the product is reminiscent of similar diphosphines that were isolated from reactions between Ph_2PX and R_2PCl or $RPCl_2$ [63–65].

The view of the solid-state structure of this diphosphine (Fig. 22) emphasizes the planarity of the cyclodiphosph(III)azane ring and the *trans* position of the phenyl groups. The phosphorus–phosphorus bond is 2.175(1) Å long, and thus almost

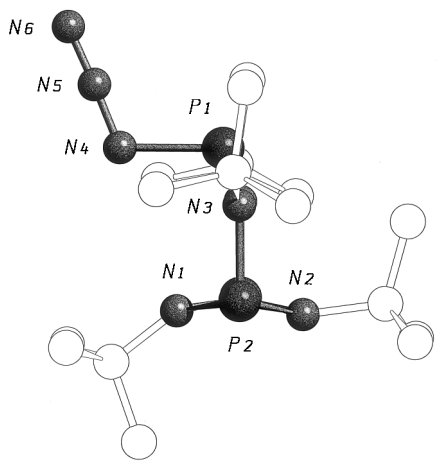

Fig. 21. Solid-state structure of [(^{t}BuNP)$_2$(^{t}BuN)$_2$PN$_3$] (**38**).

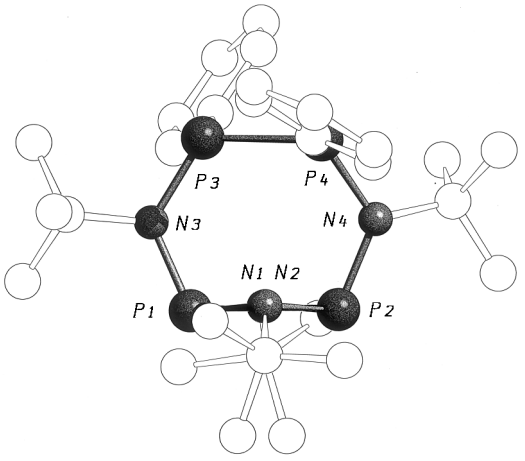

Fig. 22. Solid-state structure of $[(^tBuNP)_2(^tBuNPPh)_2]$ (**40**).

exactly twice the covalent radius of the element (1.09 Å) [24]. Surprisingly, all eight crystallographically different P–N bonds in this molecule fall in the comparatively narrow range 1.719(2)–1.753(2) Å.

5.6.2. Arsenic(III) compounds

Arsenic trichloride reacts with $[(^tBuNP)_2(^tBuNLi{\cdot}THF)_2]$ (Eq. (29)) to produce $[(^tBuNP)_2(^tBuN)_2AsCl]$ (**41**) in high yields [60]. Like the phosphorus analogue **37** this complex exhibits three singlets in its ^{1}H-NMR spectrum. A single-crystal X-ray analysis confirmed that this molecule is strictly isomorphous with **37**, with an arsenic atom that is centrally located above the cyclodiphosph(III)azane ring and forms no bonding contacts with it (Fig. 23). The arsenic–chloride bond is elongated

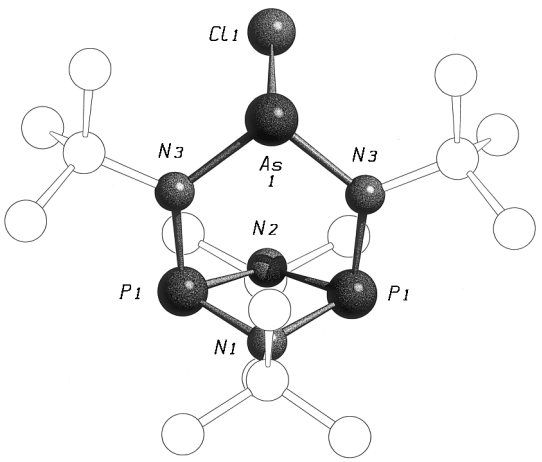

Fig. 23. Solid-state structure of $[(^tBuNP)_2(^tBuN)_2AsCl]$ (**41**).

(2.3325(11) Å), but the symmetrical arsenic–amide bonds have normal lengths (1.843(2) Å).

5.6.3. Antimony(III) compounds

The bis(amido)cyclodiphosph(III)azane compound [(^{t}BuNP)$_2$(^{t}BuN)$_2$SbCl] (**42**) is historically important, because it was the first bis(amido)cyclodiphosph(III)azane derivative of any element [20]. Perhaps as the result of an unclear reaction scheme, this tricycle has often been mislabeled as a tetrakis(trimethylsilyl)-substituted bis(amido)cyclodiphosph(III)azane compound [66–68].

Experimental details for the synthesis of **42** are vague, because they were disclosed in a communication. The reaction of antimony trichloride with (*tert*-butyl-trimethylsilylamino)(*tert*-butylimino)phosphine (Eq. (32) of Scheme 13) gen-

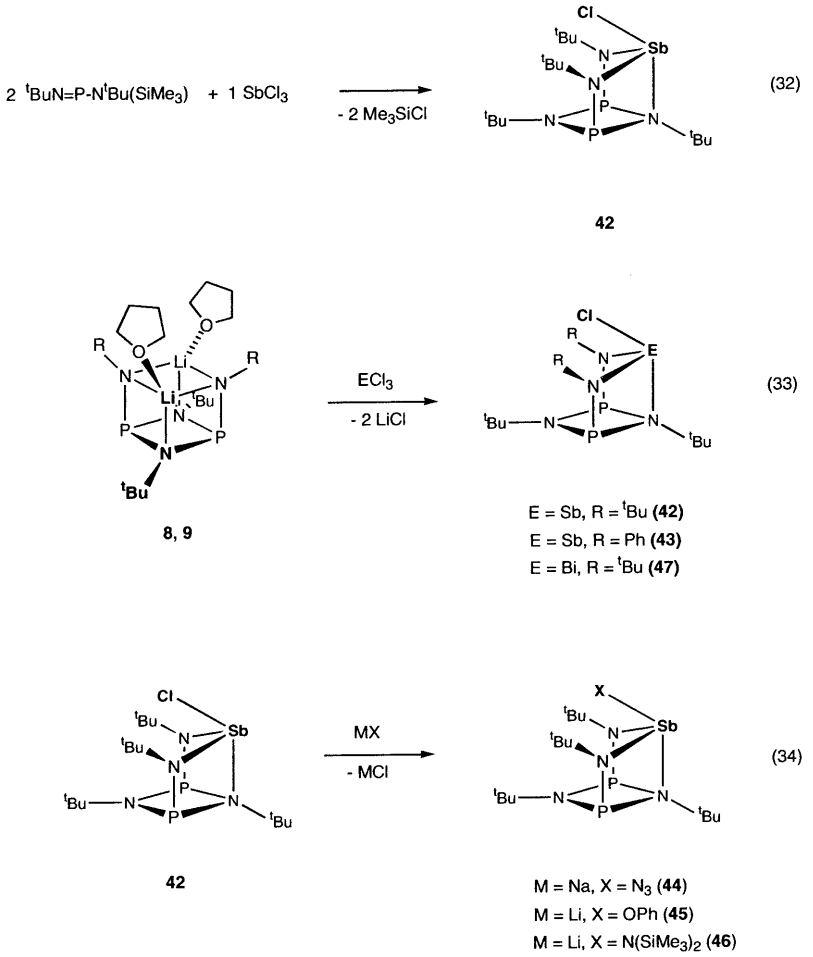

Scheme 13.

erates trimethylsilylchloride, and thus presumably proceeds via the intermediacy of an antimony species with 1,3-diaza-2-phosphaallyl ligands. It is likely that an antimony heterocycle of the type [(^{t}BuNPN^{t}Bu)$SbCl_2$] is formed initially, which then reacts with another equivalent of the amino(imino)phosphine, either to afford the intermediate [(^{t}BuNPN^{t}Bu)$_2$SbCl], or directly the product {[(^{t}BuNP)$_2$(^{t}BuN)$_2$]SbCl}. The authors claim that if the reactants are mixed in a (correct) 1:2 molar ratio, half of the amino(imino)phosphine remains unreacted, but this observation is difficult to reconcile with any obvious mechanism of ligation.

A much more straightforward synthesis for **42** was reported recently [69]. This metathesis of **8** with $SbCl_3$ (Eq. (33)) affords **42** cleanly and in 80% yield in a single-step procedure. More importantly, however, it avoids the use of the amino(imino)phosphine [^{t}BuN=P–N^{t}Bu($SiMe_3$)], which is not commercially available.

The most notable structural difference between **42** and the arsenic analogue **41**, discussed above, is the disposition of the metalloid. While the arsenic atom is located directly above the center of the $(P–N)_2$ ring, the larger antimony is displaced towards one of the imino nitrogen atoms and makes a bonding contact with it. This N–Sb donor bond is quite long (2.413(5) Å), when compared to the two covalent antimony amide bonds (2.095(5) Å). The three chemically different P–N bonds of this tricycle range from 1.680(5) Å for the exocyclic bonds to 1.772(5) Å for the endocyclic P–λ^4N bond, the latter being a typical P–N single-bond value. The antimony–chloride bond is unusually long (2.492(3) Å) when compared to the sum of the covalent radii (2.39 Å).

The ambient-temperature ^{1}H-NMR spectrum of **42** displays three singlets — one for the *tert*-butylamido groups and two for the diastereotopic *tert*-butylimino groups. The original report on the synthesis of **42** noted a concentration-dependent coalescence of these *tert*-butylimino groups and attributed it to an intermolecular chloride exchange [20]. A more recent study found no such equilibration for **42**, but suggested that those in related compounds (vide infra) were likely the result of intramolecular pyramidal inversions [69].

An analogue of **42**, namely [(^{t}BuNP)$_2$(PhN)$_2$SbCl] (**43**), prepared according to equation Eq. (33), was reported in the same paper. The unit cell of **43** contains two crystallographically independent molecules, of which only the C_s-symmetric one is shown in Fig. 24. The perspective view emphasizes this mirror symmetry of the molecule and the almost perfectly planar cyclodiphosph(III)azane ring conformation.

The monochloro compounds **42** is an excellent starting materials for derivatives, and three such species were synthesized and structurally characterized [69]. Interaction of the antimony chloride compound **42** with alkali-metal azides, phenoxides or hexamethyldisilazides (Eq. (34)) provided the corresponding azido, phenoxo and hexamethyldisilylazido compounds, respectively. X-ray studies were conducted on all three compounds and these showed that the core structures of the azide and phenoxide derivatives are almost identical to those of the chloride starting material. The hexamethyldisilazido derivative **46**, however, has a much longer antimony–nitrogen separation.

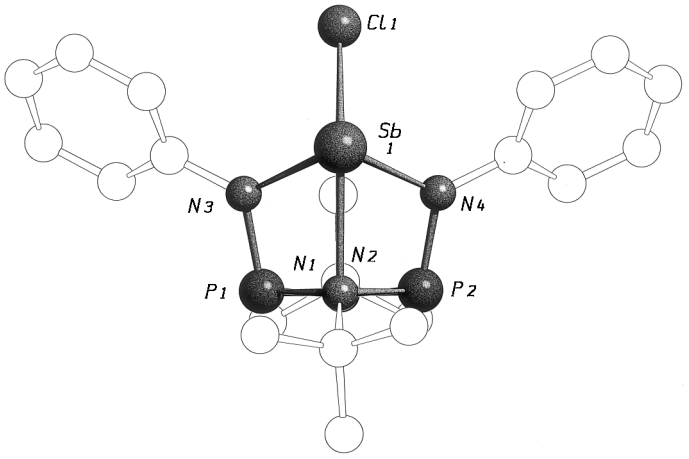

Fig. 24. Solid-state structure of [(^{t}BuNP)$_2$(PhN)$_2$SbCl] (**43**).

A view of the solid-state of the C_s-symmetric azide derivative [(^{t}BuNP)$_2$(^{t}BuN)$_2$SbN$_3$] (**44**) is shown in Fig. 25. Possibly due to the steric crowding of the azide ligand by three *tert*-butyl groups, the antimony–azide bond is unusually long (2.199(4) Å). The azide moiety is almost linear (175.8°) with N5–N6 and N6–N7 bonds of 1.196(6) and 1.145(6) Å, respectively. The cyclodiphosph(III)azane ligand coordinates the metalloid in a trihapto fashion, with symmetrical Sb–amide bonds of 2.069(4) and 2.078(4) Å, and a much longer donor bond (2.421(4) Å).

There are also two crystallographically-independent molecules in the unit cell of the phenoxide derivative [(^{t}BuNP)$_2$(^{t}BuN)$_2$SbOPh] (**45**), both of which display antimony site disorder. A view of the solid-state structure of one of these molecules is presented in Fig. 26. It shows the predominant position of the antimony atom

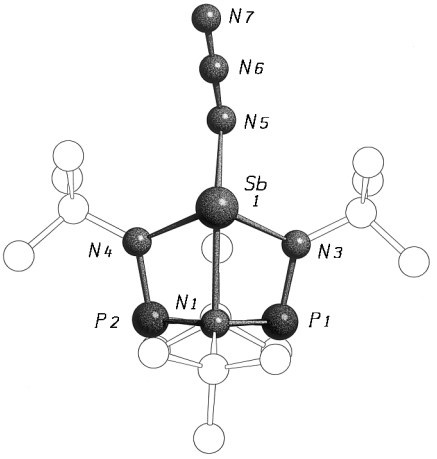

Fig. 25. Solid-state structure of [(^{t}BuNP)$_2$(^{t}BuN)$_2$SbN$_3$] (**44**).

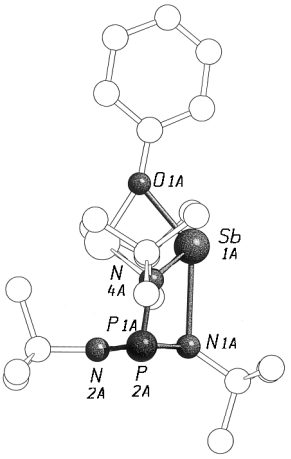

Fig. 26. Solid-state structure of [(^{t}BuNP)$_2$(^{t}BuN)$_2$SbOPh] (**45**).

shaded and the minor position in outline only. The drawing is thus quasi a composite of the two ground-state conformations of this molecule.

In contrast to the unusually long Sb–N bond in the azide derivative, the antimony–phenoxide bond has normal length (2.031(8) Å). The symmetrical antimony amide bonds are equidistant with those in **42**, while the imino–antimony donor bond is slightly longer (2.472(8) Å) than in the chloro compound.

Fig. 27 shows the solid-state structure of the hexamethyldisilazide **46** in a perspective that emphasizes the pyramidal coordination of the antimony atom. The view demonstrates that the metalloid is shielded by its ligands from all sides, but the top. Nonbonding interactions between both ligands have caused an unusually long separation between the antimony atom and the imino-nitrogen (2.656(2) Å).

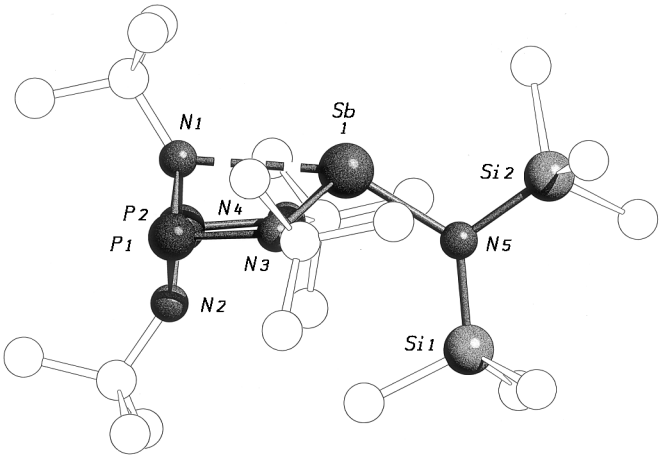

Fig. 27. Solid-state structure of [(^{t}BuNP)$_2$(^{t}BuN)$_2$SbN(SiMe$_3$)$_2$] (**46**).

5.6.4. Bismuth(III) compounds

A bismuth analogue of **42** was synthesized by a similar metathesis reaction of $BiCl_3$ with [(^{t}BuNP)$_2$(^{t}BuNLi·THF)$_2$] (Eq. (33)), albeit in much lower yields of ca. 30% [69]. The bright orange [(^{t}BuNP)$_2$(^{t}BuN)$_2$BiCl] (**47**) has a structure similar to that of **42**, but disorder in the solid-state prevented a publication of the X-ray studies.

At room temperature only two singlets were observed in the ^{1}H-NMR spectrum, indicative of a fluxional molecule. Upon cooling one of these signals coalesced and reemerged as two widely separated singlets. Activation parameters for this exchange were obtained by variable-temperature NMR studies and these are discussed below.

5.6.5. Pyramidal inversion in Group 15 bis(amido)cyclodiphosph(III)azane compounds

Just like their mononuclear Group 13 analogues discussed above, the Group 15 bis(amido)cyclodiphosph(III)azane compounds have C_s symmetry. The concomitant diastereotopicity should render the *tert*-butylimino groups magnetically distinct, and indeed two signals are usually observed in the ^{1}H-NMR spectra.

Only a rapid pyramidal inversion by the central Group 15 element can equilibrate the two *tert*-butyl substituents. This type of fluxionality is different from that shown by the Group 13 compounds, in which mere bond fluctuations are required to make both imino substituents equivalent. Pyramidal inversions typically have higher activation barriers than other molecular rearrangements and only those of tertiary amines are readily surmountable at room temperature.

Variable-temperature ^{1}H-NMR studies allowed the calculation of activation energies for **43** and **47**, and the estimation of minimal activation energies for all others, using certain simplifying assumptions.

Based on these studies, the bismuth derivative **47** has a $\Delta G^{\ddagger}$ of 54 kJ mol^{-1}, while the antimony analogue **43** has a much higher barrier of ca. 75 kJ mol^{-1}. All other Group 15 compounds have free energies of activation of at least 100 kJ mol^{-1} and in some cases substantially higher values. These $\Delta G^{\ddagger}$ follow normal trends in pyramidal inversions of Group 15 compounds [33], showing that the inclusion of Group 15 elements in these tricyclic compounds does not change their order of activation energies.

6. Summary and conclusions

While cyclodiphosph(III)azanes have been known for more than 100 years, their coordination chemistry as amide ligands is less than 15 years old and has been actively investigated for only about 5 years. In this relatively short period, however, it has been possible to incorporate elements from almost all main-groups in these ligands. The data presented above reflect the comparative novelty of this topic, because most studies have focused on syntheses and structures of these compounds. This emphasis on the basics, however, has led to a rapid expansion of this topic and a good understanding of the ways these heterocycles chelate a wide variety of chemical elements.

The synthetic studies described above have shown that bis(amino)cyclodiphosph(III)azanes are remarkably versatile *N*-donor ligands that allow the incorporation of main-group metals, metalloids and nonmetals from almost any area of the periodic table. Elements as small as boron and as large as bismuth, with oxidation states ranging from $+1$ to $+4$, form mono- or dinuclear compounds with these ligands.

The ensuing compounds have highly symmetrical bicyclic or tricyclic structures. This symmetry, which is never less than C_s, is reflected in simple NMR spectra, molecular fluxionality, and the occasional static disorder in the solid state.

All of the bi- and tricycles for which X-ray data are available adopt one of the structures **I**–**III**, shown in Scheme 4. In these compounds two or three, but never just one or four, of the bis(amido)cyclodiphosph(III)azane ligand's nitrogen atoms form bonds with one main-group element. Only in the dinuclear compounds of lithium and thallium are all nitrogen atoms involved in metal coordination.

Single elements are invariably coordinated in either a di- or trihapto fashion, with one of the η^3-coordinated ligand's bond being a donor bond from an imino-nitrogen atom. This trihapto chelation is the most common coordination variant for main-group compounds of the ligand, but the degree to which the donor bond is developed varies greatly from complex to complex, and in many cases the extent of the bonding is not easy to determine. As a result of its inclusion in a bicyclic compound the main-group element is often forced to be in close contact with the imino-nitrogen atoms, making the separation of central element and imino-nitrogen a poor indicator of bond strength. This is particularly evident in the activation energies of Group 13 compounds, which are less than 40 kJ mol^{-1}, despite comparatively short donor bonds.

Their unusual structural properties set bis(amido)cyclodiphosph(III)azanes apart from conventional chelating bis(amido) ligands. They have wider girths than most amide ligands and can thus more completely envelop the chelated element. Consequently, they do not require extremely bulky amido substituents to prevent dimerization of their compounds. Cyclodiphosph(III)azanes provide an excellent size match for many elements, especially the larger ones, like tin and thallium. This fit is reflected in nonbonding intramolecular E–P contacts that are almost always much closer than the sum of the van der Waals radii of the elements.

Many pristine *cis*-bis(amino)cyclodiphosph(III)azanes are puckered with a noticeable 'W'-shaped ring conformation, in which the imino-nitrogen lie above the ring's least-squares plane. In their compounds, however, cyclodiphosph(III)azanes have more planar rings, whose puckering is often the result of nonbonding interactions with exocyclic ligands, or between central element and the four-membered ring. Bicyclic or polycyclic compounds that do show puckering have cyclodiphosph(III)azane rings in which the nitrogen atoms lie below, rather than above, the least-squares plane. The ring portion of the ligand has thus been pushed out, much like the bottom of a brown bag.

Reactivity studies of main-group bis(amido)cyclodiphosph(III)azane compounds are in their early stages. Transition metal compounds of bis(amido)cyclodiphosph(III)azanes have shown good activity as polyolefin catalysts [1], and unusual

reactivity patterns can also be expected from some of the main group derivatives.

These studies on the coordination chemistry of bis(amido)cyclodiphosph(III)azanes may help unravel some of the mechanisms by which these heterocycles form and interconvert. The isolation of the aluminate complex **14** and the antimony compound **42** shows that the ligand can be formed in the coordination sphere of the metal. The opposite of this cycloaddition, namely cycloreversion, was observed in the reaction of neutral bis(amino)cyclodiphosph(III)azanes with *n*-butyllithium, and the reaction of gallium chloride with the dilithio salt **8**.

The success of bis(amido)cyclodiphosph(III)azanes as ligands raises the question to what extent their higher homologues, cyclodiarsazanes and cyclodistibazanes, can function in a similar role. Arsenic analogues of some of the bis(amino)cyclodiphosph(III)azanes discussed above already exist [70,71], as do some of their compounds [72]. While the toxicity of these ligands will prevent their use as catalysts, main-group compounds of cyclodiarsazanes are promising materials precursors

Cyclodistibazanes are known as well [72,73], but those that have been isolated are more thermally labile than their phosphorus and arsenic analogues. Bis(1°-amino)cyclodistibazanes cannot be prepared cleanly, because of their facile transformation to the corresponding trinuclear antimony compounds [73], making the development of a parallel stibazane coordination chemistry improbable.

Acknowledgements

In collecting these data I have relied on reports from chemists in laboratories around the world. I am grateful to these researchers, whose names appear in the reference section, for their diligence in helping elucidate the chemistry of bis(amino)cyclodiphosph(III)azanes and their bicyclic and tricyclic main-group compounds. I also thank the University of North Dakota for a Summer Professorship.

References

[1] (a) L. Grocholl, V. Huch, L. Stahl, R.J. Staples, P. Steinhart, A. Johnson, Inorg. Chem. 36 (1997) 4451. (b) L. Grocholl, L. Stahl, R.J. Staples, J. Chem. Soc. Chem. Commun. (1997) 1465.
[2] See, for example: F.A. Cotton, G. Wilkinson, C.A. Murillo, M. Bochmann, Advanced Inorganic Chemistry, fifth ed., Wiley, New York, 1999, p. 347.
[3] I. Haiduc, D.B. Sowerby, The Chemistry of Inorganic Homo- and Heterocycles, vol. I and II, Academic Press, London, 1987.
[4] U. Klingebiel, in: The Chemistry of Inorganic Homo- and Heterocycles, vol. I, Academic Press, London, 1987, pp. 221–269.
[5] M. Veith, S. Becker, V. Huch, Angew. Chem. Int. Ed. Engl. 29 (1990) 216.
[6] R.H. Neilson, P. Wisian-Neilson, Chem. Rev. 88 (1988) 541. (b) C.W. Allen, Coord. Chem. Rev. 130 (1994) 137.

[7] C.W. Allen, in: The Chemistry of Inorganic Homo- and Heterocycles, vol. II, Academic Press, London, 1987, pp. 501–589.
[8] R. Keat, in: The Chemistry of Inorganic Homo- and Heterocycles, vol. II, Academic Press, London, 1987, pp. 467–496.
[9] R. Keat, Top. Curr. Chem. 102 (1982) 89.
[10] A.D. Norman, Main Group Chem. News 4 (1996) 25.
[11] (a) M. Michaelis, G. Schroeter, Chem. Ber. 27 (1894) 490. (b) M. Michaelis, Annalen 326 (1903) 129.
[12] (a) R.R. Holmes, J.A. Forstner, Inorg. Chem. 2 (1963) 380. (b) R.R. Holmes, J. Am. Chem. Soc. 83 (1961) 1334.
[13] R. Jefferson, J.F. Nixon, T.M. Painter, J. Chem. Soc. Chem. Commun. (1969) 622.
[14] K.W. Muir, J.F. Nixon, J. Chem. Soc. Chem. Commun. (1971) 1405.
[15] E. Niecke, W. Flick, S. Pohl, Angew. Chem. Int. Ed. Engl. 15 (1976) 309.
[16] O.J. Scherer, G. Schmidt, Angew. Chem. Int. Ed. Engl. 15 (1976) 772.
[17] M.L. Thompson, A. Tarassoli, R.C. Haltiwanger, A.D. Norman, J. Chem. Soc. Chem. Commun. (1979) 647.
[18] R. Jefferson, J.F. Nixon, T.M. Painter, R. Keat, L. Stobbs, J. Chem. Soc. Dalton Trans. (1973) 1414.
[19] L.N. Markovskii, V.D. Romanenko, A.V. Ruban, L.A. Robenko, Zh. Obshch. Khim. 50 (1979) 337.
[20] O.J. Scherer, G. Wolmershäuser, H. Conrad, Angew. Chem. Int. Ed. Engl. 22 (1983) 404.
[21] M.S. Balakrishna, V. Sreenivasa Reddy, S.S. Krishnamurthy, J.F. Nixon, J.C.T.R. Burckett St. Laurent, Coord. Chem. Rev. 129 (1994) 1.
[22] (a) V. Sreenivasa Reddy, S.S. Krishnamurthy, M. Nethaji, J. Chem. Soc. Dalton Trans. (1995) 1933. (b) S.S. Krishnamurthy, V. Sreenivasa Reddy, A. Chandrasekaran, M. Nethaji, Phosphorus Sulfur Silicon 64 (1994) 99.
[23] (a) N.D. Reddy, A.J. Elias, A. Vij, J. Chem. Soc. Dalton Trans. (1997) 2167. (b) I. Schranz, L. Stahl, R.J. Staples, Inorg. Chem. 37 (1998) 1493.
[24] D.E.C. Corbridge, Phosphorus: An Outline of its Chemistry, Biochemistry and Technology, fifth ed., Elsevier, Amsterdam, 1995.
[25] (a) A. Tarassoli, R.C. Haltiwanger, A.D. Norman, Inorg. Chem. 21 (1982) 2684. (b) M.L. Thompson, A. Tarassoli, R.C. Haltiwanger, A.D. Norman, Inorg. Chem. 26 (1987) 684.
[26] O.J. Scherer, P. Klusmann, Angew. Chem. Int. Ed. Engl. 8 (1969) 752.
[27] H.-J. Chen, R.C. Haltiwanger, T.G. Hill, M.L. Thompson, D.E. Coons, A.D. Norman, Inorg. Chem. 24 (1985) 4725.
[28] A.R. Davies, A.T. Dronsfield, R.N. Haszeldine, D.R. Taylor, J. Chem. Soc. Perkin Trans. I (1973) 379.
[29] D.F. Moser, L. Stahl, unpublished results.
[30] K.W. Muir, J. Chem. Soc. Dalton Trans. (1975) 259.
[31] D.F. Moser, L. Stahl, unpublished results.
[32] I. Silaghi-Dumitrescu, I. Haiduc, Phosphorus Sulfur Silicon 91 (1994) 21.
[33] (a) L. Horner, H. Winkler, Tetrahedron Lett. (1964) 461. (b) G.H. Senkler Jr., K. Mislow, J. Am. Chem. Soc. 94 (1972) 291.
[34] I. Silaghi-Dumitrescu, F. Lara-Ochoa, I. Haiduc, Main Group Chem. 2 (1998) 309.
[35] W. Wirringa, H. Voelker, H.W. Roesky, Y. Shermolovich, L. Markovski, I. Usón, M. Noltemeyer, H.-G. Schmidt, J. Chem. Soc. Dalton Trans. (1995) 1951.
[36] I. Schranz, D.F. Moser, L. Stahl, R.J. Staples, Inorg. Chem. 38 (1999) 5814.
[37] G. Linti, H. Nöth, E. Schneider, W. Storch, Chem. Ber. 126 (1993) 619.
[38] A. Streitwieser, Jr., C.H. Heathcock, Introduction to Organic Chemistry, Macmillan, New York, 1976, p. 775.
[39] M.A. Beswick, A.J. Edwards, J.R. Galsworthy, M.A. Paver, R.R. Raithby, M.-A. Rennie, C.A. Russell, K.L. Verhorevoort, D.S. Wright, Inorg. Chim. Acta 248 (1996) 9.
[40] J.K. Brask, T. Chivers, M.L. Krahn, M. Parvez, Inorg. Chem. 38 (1998) 298.

[41] M. Veith, F. Goffing, V. Huch, Chem. Ber. 121 (1988) 943.
[42] L. Grocholl, L. Stahl, unpublished results.
[43] P.B. Hitchcock, H.A. Jasmin, M.F. Lappert, H.D. Williams, J. Chem. Soc. Chem. Commun. (1986) 1634.
[44] R. Detsch, E. Niecke, M. Nieger, W.W. Schoeller, Chem. Ber. 125 (1992) 1119.
[45] G. Fink, R. Mülhaupt, H.H. Brintzinger (Eds.), Ziegler Catalysts, Springer, Berlin, 1995.
[46] M. Bochmann, J. Chem. Soc. Dalton Trans. (1996) 255
[47] M.R. Mason, J.M. Smith, S.G. Bott, R. Barron, J. Am. Chem. Soc. 115 (1993) 4971.
[48] M.P. Coles, R.F. Jordan, J. Am. Chem. Soc. 119 (1997) 8125.
[49] M. Reinhold, J.E. McGrady, R.J. Meier, J. Chem. Soc. Dalton Trans. (1999) 487.
[50] N. Burford, D.J. LeBlanc, Inorg. Chem. 38 (1999) 2248.
[51] D.F. Moser, L. Stahl, unpublished results.
[52] L. Grocholl, I. Schranz, L. Stahl, R.J. Staples, Inorg. Chem. 37 (1998) 2496.
[53] M. Veith, F. Goffing, S. Becker, V. Huch, J. Organomet. Chem. 406 (1991) 105.
[54] S.S. Kumaravel, S.S. Krishnamurthy, T.S. Cameron, A. Linden, Inorg. Chem. 27 (1988) 4546.
[55] R. Keat, D.G. Thompson, J. Chem. Soc. Dalton Trans. (1980) 928.
[56] I. Schranz, L. Stahl, unpublished results.
[57] I. Schranz, M.S. Thesis, University of North Dakota, ND, USA, 1998.
[58] M. Veith, S. Becker, V. Huch, Angew. Chem. Int. Ed. Engl. 28 (1989) 1237.
[59] T.G. Hill, R.C. Haltiwanger, M.L. Thompson, S.A. Katz, A.D. Norman, Inorg. Chem. 33 (1994) 1770.
[60] I. Schranz, L.P. Grocholl, L. Stahl, R.J. Staples, A. Johnson, Inorg. Chem. 39 (2000).
[61] (a) G. Bertrand, J.-P. Majoral, A. Baceiredo, Acc. Chem. Res. 19 (1986) 17. (b) A. Baceiredo, G. Bertrand, J.-P. Majoral, G. Sicard, J. Jaud, J. Galy, J. Am. Chem. Soc. 106 (1984) 6088.
[62] A.H. Cowley, F. Gabbaï, R. Schluter, D. Atwood, J. Am. Chem. Soc. 114 (1984) 3144.
[63] R. Schmutzler, Z. Naturforsch. 44b (1989) 690.
[64] H.W. Roesky, K. Ambrosius, W.S. Sheldrick, Chem. Ber. 112 (1979) 1365.
[65] L. Meinel, H. Nöth, Z. Anorg. Allg. Chem. 349 (1967) 225.
[66] E. Niecke, in: M. Regitz, O. Scherer (Eds.), Multiple Bonds and Low Coordination in Phosphorus Chemistry, Thieme, Stuttgart, 1990, p. 293.
[67] M. Witt, H.W. Roesky, Chem. Rev. 94 (1994) 1163.
[68] E. Niecke, D. Gudat, Angew. Chem. Int. Ed. Engl. 30 (1991) 217.
[69] D.F. Moser, I. Schranz, M.C. Gerrety, L. Stahl, R. Staples, J. Chem. Soc. Dalton Trans. (1999) 751.
[70] (a) H.-J. Vetter, H. Strametz, H. Nöth, Angew. Chem. 75 (1963) 417. (b) H.-J. Vetter, H. Nöth, W. Jahn, Z. Anorg. Allg. Chem. 144 (1964) 144. (c) H.-J. Vetter, H. Nöth, Z. Naturforsch. 19b (1964) 167.
[71] R. Bohra, H.W. Roesky, M. Noltemeyer, G.M. Sheldrick, Acta Crystallogr. C40 (1984) 1150.
[72] M. Veith, A. Rammo, M. Hans, Phosphorus Sulfur Silicon 93–94 (1994) 197.
[73] R.A. Alton, D. Barr, A.J. Edwards, M.A. Paver, P.R. Raithby, M.-A. Rennie, C.A. Russell, D.S. Wright, J. Chem. Soc. Chem. Commun. (1994) 1481.